ADVANCED THERAPEUTICS
www.advtherap.com

Hybrid Nanoparticles Dual-Loaded With Curcumin and Benzydamine Hydrochloride for the Treatment of Vulvovaginal Candidiasis: From Development to Biological Application In Vitro and In Vivo

Gabriela C. Carvalho, Maria Nolasco Viseu Domingues, Gabriel Davi Marena, Ermei Mäkilä, Jiachen Li, Gésinda Geertsema-Doornbusch, Cleverton Roberto de Andrade, Marc C. A. Stuart, Mohammad-Ali Shahbazi, Ione Corrêa, Brandon W. Peterson, Jarno Salonen, Helena F. Florindo, Taís Maria Bauab, Marlus Chorilli, and Hélder A. Santos**

Vulvovaginal candidiasis represents a public health challenge due to its reports of high incidence and recurrence. These are caused by host-related factors like compromised immune system, or pathogen-related factors, such as resistance to antifungal agents, making this medical problem desirable to develop new therapeutic options. In this context, natural origin substances like curcumin, are increasingly treatment alternatives. However, some curcumin properties limit its therapeutic application, such as insolubility in aqueous solvents, which leads to low bioavailability. Nevertheless, nanotechnology association with drugs of plant origin proves to be a promising alternative to overcome the reported drawbacks. Despite being caused by a fungus, patients suffer significantly from the inflammation resulting from this disease, thus this study aimed to develop a hybrid carrier nanoformulation by microfluidics loaded with two drugs, benzydamine hydrochloride (an anti-inflammatory drug) and curcumin (an antifungal drug). Transmission electron cryomicroscopy combined with energy dispersive X-ray analysis confirmed that the nanoparticle is properly developed. Through in vitro biological studies, it is possible to observe that, in addition to being safe, the encapsulation of both drugs in the nanocarrier drastically reduced their cytotoxicity. Finally, although the final nanoformulation does not show in vitro activity, the in vivo study indicated therapeutic potential.

1. Introduction

Vulvovaginal candidiasis (VVC) is an infection in the vulva region caused by the fungus *Candida* sp., which is considered a public health problem since it is the second leading cause of vaginitis. While there is a lack of updated global prevalence data for this disease, its prevalence can be observed through studies carried out in specific countries, like 18% in Brazil,[1] 33% in sub–Saharan Africa[2] 22.8% in Taiwan and 15.5 and 14% in Belgium on summer and winter respectively.[3] Despite the wide range of available drugs, literature reports ineffective treatments attributed to fungus resistance to several drugs used in therapy. Those ineffective treatments may result in complications, such as pelvic abscess, pelvic inflammatory disease, infertility and miscarriage, underscoring the clinical importance of studying new therapeutic options.[4–7] In this context, an increasing amount of research is being done in order to overcome this resistance issue. For example, new strategies associating drugs

G. C. Carvalho, G. D. Marena, T. M. Bauab, M. Chorilli
School of Pharmaceutical Sciences
São Paulo State University (UNESP)
Rodovia Araraquara Jaú, Km 01 - s/n - Campos Ville, Araraquara 14800–903, Brazil
E-mail: marlus.chorilli@unesp.br

The ORCID identification number(s) for the author(s) of this article can be found under https://doi.org/10.1002/adtp.202400342

DOI: 10.1002/adtp.202400342

G. C. Carvalho, M. N. V. Domingues, J. Li, G. Geertsema-Doornbusch, M.-A. Shahbazi, B. W. Peterson, H. A. Santos
Department of Biomaterials and Biomedical Technology, The Personalized Medicine Research Institute (PRECISION), University Medical Center Groningen
University of Groningen
Ant. Deusinglaan 1, Groningen, AV 9713, The Netherlands
E-mail: h.a.santos@umcg.nl

M. N. V. Domingues, H. F. Florindo
Research Institute for Medicines (iMed.ULisboa), Faculdade de Farmácia
Universidade de Lisboa
Av. Prof. Gama Pinto, Lisbon 1649-003, Portugal

already well established in therapeutics, such as chitosan-based sponges containing clotrimazole[8] and stimuli-responsive in situ miconazole nitrate spray gel.[9] As well as exploring others active molecules, like ibrexafungerp[10] and natural products.[11] Plant-based alternatives, such as curcumin (CUR), have been gaining attention.

This compound, a yellow polyphenol and hydrophobic bioactive extracted from the *Curcuma longa L* rhizome, has several pharmacological properties, including anti-inflammatory and antifungal actions, especially against *Candida* sp.[12–14] This drug was selected here since several studies in the literature pointed to its therapeutic efficiency against Candida infections, specially VVC.[15–17] However, CUR is insoluble in aqueous solvents, which leads to low bioavailability, hindering its use in therapy.[18,19] The association of nanotechnology with drugs of plant origin with low solubility in aqueous media proves to be a promising alternative.[20–22] Although antifungals of natural origin are considered efficient to overcome some limitations, such as resistance and conventional therapy adverse effects, it may not be sufficient in the case of symptomatic patients. This is because, in addition to the infection, these patients also have the recruitment of polymorphonuclear leukocytes (PMN) in the vaginal lumen, causing acute symptoms. Therefore, the association of antifungals with anti-inflammatory drugs is an interesting strategy for the treatment of those patients.[23,24]

In addition to CUR, it is worth mentioning benzydamine hydrochloride (BNZ), a synthetic nonsteroidal anti-inflammatory drug.[25,26] This drug is widely used for topical applications, and it is possible to observe several articles in the literature where it was used to treat VVC. Furthermore, it is the active component of several formulations marketed worldwide for the treatment of gynecological conditions. In addition to this activity, BNZ also has well-documented antifungal activity, which makes it an ideal drug for VVC treatment.[26–28] It is worth mentioning that, to the best of our knowledge, this study is the first one to propose this innovative drug association.

Among the various systems used for drug delivery, lipid-based ones, like liposomes, can be highlighted as it is one of the most widely used systems in the world. This popularity is attributed to advantages like excellent biocompatibility, customizable size, easy surface modulation, drug protection from degradability, ability to control the release of incorporated drugs, and high retention of drug loads at the action site.[29–31] This type of system consists of spherical vesicles containing one or more lipid bilayers. Since it has hydrophobic and hydrophilic properties, it exhibit versatility to incorporate both, hydrophobic (inside the lipid bilayer) and hydrophilic molecules (in the core).[32]

A second system that is also considered promising and needs to be highlighted is the mesoporous silica nanoparticle (MSNs). These nanoparticles stands out due to their widely application for biomedicine purposes and desirable properties, such as large surface area, high chemical and thermal stability, tunable particle diameter and pore structure, free hydroxyl groups for functionalization, biodegradability, biocompatibility, low toxicity, and easy elimination from organisms.[33–35] Although there is a considerable amount of research involving MSNs, only one formulation has been approved by the Food and Drug Administration (FDA) for clinical trials to date. In this sense, hybrid nanoparticles, combining MSNs with lipids or natural polymers for example, have been considered an alternative to bring this type of material closer to its application in therapy as those materials make silica more biomolecule-friendly and stable, in addition to provide a barrier against premature drug release and increase its circulation time in the body.[36,37]

Thus, aiming to design, by microfluidics, a novel nanoparticle system, which would allow controlled and prolonged antifungal and anti-inflammatory action of CUR and BNZ, a hybrid nano-in-nano (NIN) formulation was proposed. The strategy was to incorporate one drug into the lipid bilayer of a liposome-like structure and the other into the MSNs, which would be encapsulated as the core of this liposome. Although there are studies in the literature describing the development of hybrid nanoparticles combining these two types of materials,[36,38–40] the use of microfluidics to synthetize them, according to our knowledge of the literature, gives an innovative character to this study. This cutting edge synthesis method is proposed here because although conventional bulk methods for nanoparticle synthesis have a broad history of application and are considered suitable for the intended purpose, when production quantity increase is wanted conventional methods show the limitation of not being scalable, mainly due to the lack of reproducibility.[41] In response to this, the microfluidics technique is increasingly gaining ground because through precise control of chemical reactions conditions and the flow of multiphase fluids, it is possible to establish a reproducible, controllable and easily scalable methodology. Furthermore, this technique favors a higher loading degree compared to conventional bulk methods.[42,43] It is worth highlighting that for each different type of nanoparticle that is intended to be obtained, there is a different microfluidics device to be chosen (made by different materials like polymers, silicone or paper). Aiming the production of liposome-like particles it is worth mentioning the microfluidic hydrodynamic flow focusing, a laminar flow method in which a narrow fluid flows in a channel within a different fluid.[41]

In the process of developing a formulation, it is important to dedicate effort to the appropriate choice of the administration route, once an inadequate route can compromise the treatment effectiveness.[44] Despite being considered alternative the vaginal

E. Mäkilä, J. Salonen
Laboratory of Industrial Physics, Department of Physics and Astronomy
University of Turku
Vesilinnantie 5, Turku 20500, Finland
C. R. de Andrade
Araraquara Dental School
São Paulo State University (UNESP)
Humaitá, 1680, Araraquara 14801-385, Brazil
M. C. A. Stuart
Groningen Biomolecular Sciences and Biotechnology Institute
University of Groningen
Nijenborgh 7, Groningen 9747 AG, The Netherlands
I. Corrêa
Medical School
São Paulo State University (UNESP)
Av. Prof. Mário Rubens Guimarães Montenegro, s/n, Botucatu 18618687, Brazil
H. A. Santos
Drug Research Program, Division of Pharmaceutical Chemistry and Technology, Faculty of Pharmacy
University of Helsinki
Viikinkaari 5, Helsinki FI-00014, Finland

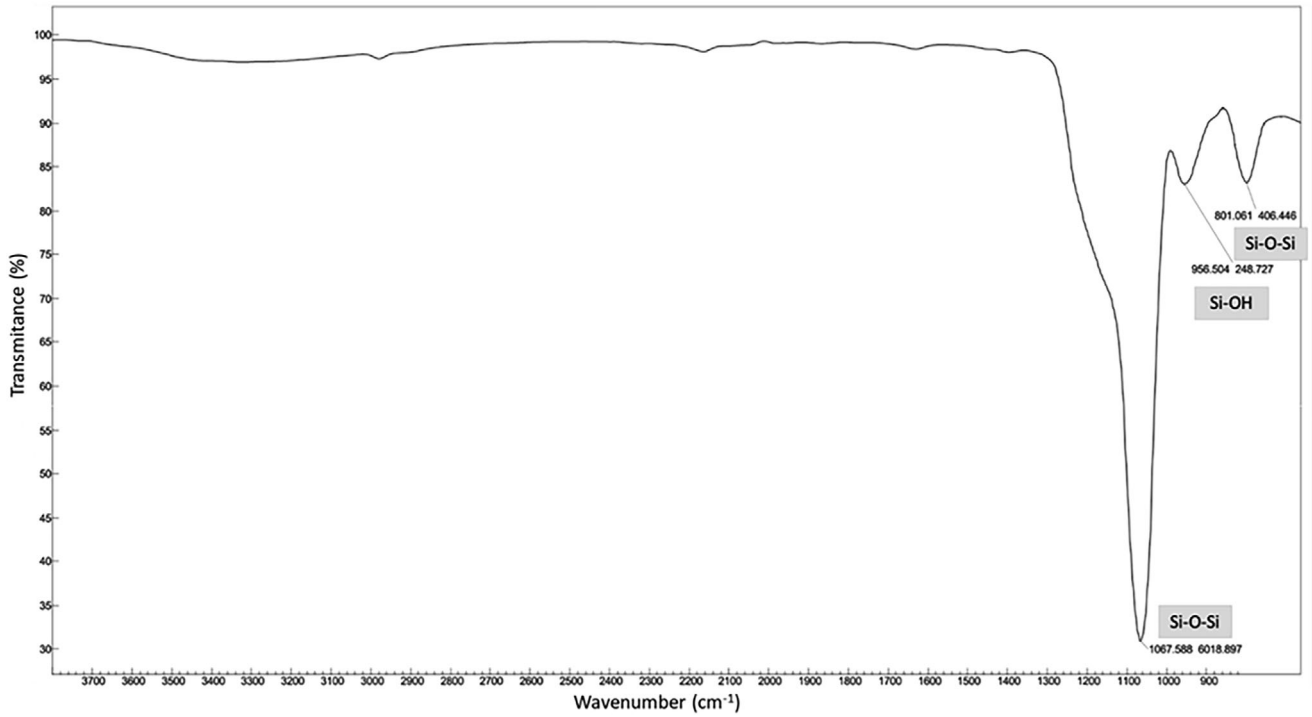

Figure 1. Representative bare of the mesoporous silica nanoparticle Fourier-transform infrared spectroscopy spectrum baseline corrected. The characteristic bands of the silica matrix were indicated as well as its respective exactly wavenumber.

route stands out mainly when a local effect is wanted, like in the case of VVC treatment, once it can bypass first-pass metabolism, decrease adverse effects and drug interactions.[45,46] Nevertheless, considering the challenge of a smart administration, it is worth mentioning that due the vaginal anatomy semi-solid formulations are difficult to apply, and liquids formulations can cause discomfort to the patient as they can quickly disperse and leak from the application site. An interesting alternative for the aforementioned is the use of thermo-responsive and mucoadhesive hydrogels. Thermo-responsive formulations, like poloxamer-based ones, can be liquid at room temperature (so easy to apply) and gel at body temperature (having the ability to remain in the administration place), bypassing these limitations.[1,47,48] In addition to this mucoadhesive formulations, like chitosan-based ones, has the ability to interact with the vaginal mucosa remaining adhered to the vaginal cavity for longer time than formulations that do not have this property.[49]

In the present work, we sought to develop and evaluate a NIN system incorporated with CUR and BNZ, one in each part of the nanoparticle (MSNs and lipid bilayer) dispersed in thermoresponsive and mucoadhesive hydrogel and evaluate its antifungal and anti-inflammatory biological activity, in vitro and in vivo, against VVC.

2. Results and Discussion

2.1. MSNs Synthesis and Characterization

According to the dynamic light scattering (DLS) analysis, the MSNs had an average hydrodynamic size of 140.8 nm, with a polydispersity index (PDI) of 0.213 and zeta potential of −23.4 mV, indicating good size distribution, and charge, similar to previous reports.[50–53]

In order to confirm that the silica matrix had been formed, Fourier-transform infrared spectroscopy (FTIR) analysis was first performed. In **Figure 1** it is possible to observe bands in the regions of 800 and 1085 cm^{-1} corresponding to symmetrical and asymmetrical axial stretching of Si-O-Si respectively, which is characteristic of the silica matrix. Furthermore, the band around 960 cm^{-1} can be attributed to an axial Si-OH stretching, which can be due to the silanols groups available on the surface and inside the MSNs pores.[54–56]

Subsequently, in order to verify whether the acid reflux process was capable of removing the organic matter (making the pores free for drug incorporation), a stepwise thermogravimetric (TG) analysis was carried out. **Figure 2A** represents the TG graph of weight versus temperature (Figure S1, Supporting Information represents the TG weight vs temperature vs time graph). It is possible to observe that initially there is a weight loss (9.2 wt% of the initial weight) related to humidity and water bound in two stages. The first one is due to the weakly adsorbed water from the environment that was almost completely removed at 35 °C, while the second one is due the hydrogen-bonded water removed at 120 °C.[57] Subsequently, there is a small weight loss (approximately 0.72%) starting at 495 °C, possibly due to the remaining residue of the pore templating agent or other organic impurities left from the synthesis process.[57,58]

Surface area and pore size distribution were analyzed by nitrogen sorption measurement. It was observed that the obtained nanoparticles have a specific surface area of 762 m^2/g

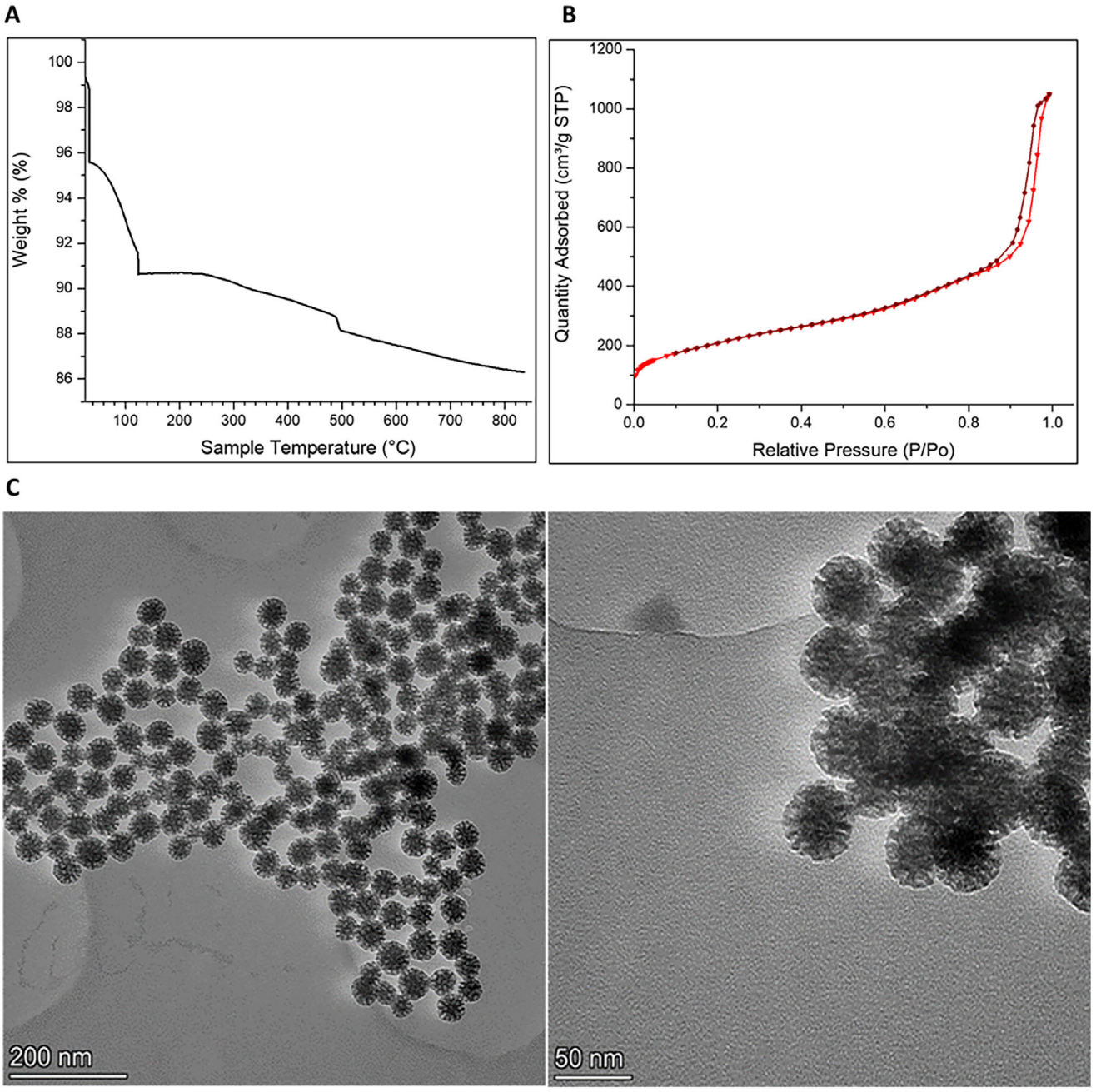

Figure 2. Representatives bare of the mesoporous silica nanoparticle A) Thermogravimetric weight loss curve; B) Brunauer-Emmett-Teller adsorption-desorption isotherm graph; C) Transmission electron microscopy micrographs.

and an estimated pore volume of 1.58 cm^3 g^{-1}, with a type IV adsorption-desorption isotherm, as shown in Figure 2B.[59] Pore size distribution calculation shows 2 to 4 nm cylindrical pores, as well as some 7 nm pores. Finally, the samples were characterized by transmission electron microscopy (TEM) and Figure 2C shows that the MSNs have a spherical shape, with ≈50 nm in size and suggestive mesopores structures, which reinforces the Brunauer-Emmett-Teller (BET) findings described above.

2.2. Hybrid Nanoparticle System Development and Characterization

The formation of the NIN by microfluidics was possible with the flow condition of 9 and 1 mL/h for the inner and outer phases, respectively. **Figure** 3A and B compare the transmission electron cryomicroscopy (Cryo-TEM) images of bare MSNs and NIN, where it is possible to observe the lipid bilayer surrounding the MSNs. It is also possible to observe that the nanoparticles are

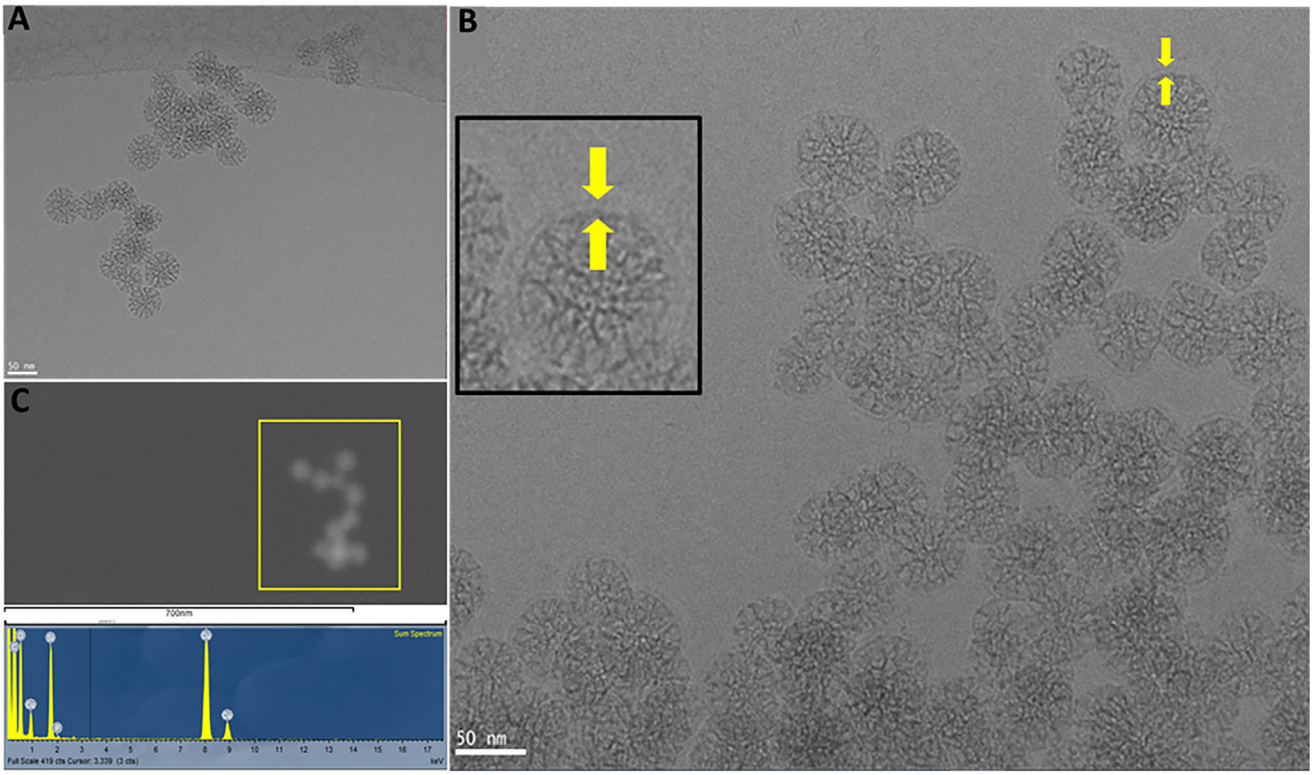

Figure 3. Nano-in-nano characterization results. A) Representative transmission electron cryomicroscopy images of the bare mesoporous silica nanoparticle;B) Representative transmission electron cryomicroscopy images of the nano-in-nano (yellow arrows indicate the lipid-bilayer); C) Energy dispersive X-ray analysis of the elemental composition of the nano-in-nano.

homogeneous, which indicates the obtention of monodisperse hybrid nanoparticles. The presence of the lipid bilayer was further confirmed with energy dispersive X-ray (EDX). The obtained spectra from the area, shown in Figure 3C, indicates the presence of phosphorus from the phosphatidylcholine in the NIN system.

From the Cryo-TEM images it is also possible to observe that after the lipid coverage the nanoparticles maintained their spherical shape but increased in size, from 50 nm to *ca.* 70 nm. By DLS, an increase in the average hydrodynamic diameter was also observed, from 140.8 nm (MSNs) to 208.8 nm (NIN). Furthermore, a change in zeta potential was also noted, from −23.4 to −5.31 mV. The zwitterionic character of the phosphatidylcholine group present in both lipids gives to the nanoparticles a charge closer to neutral.[60,61]

Regarding the numerical analyses, the Reynolds number obtained was 40, which indicates that the viscous forces overwhelm inertial forces resulting in fluids in laminar flow (<<2300).[62,63]

Table 1. Comparison between the minimal inhibitory concentration of curcumin and benzydamine hydrochloride alone and their combination against a clinical resistant *Candida albicans* strain.

Drug	MIC_{90} alone	MIC_{90} combined
CUR	62.5 μg mL^{-1}	19.5 μg mL^{-1}
BNZ	125.0 μg mL^{-1}	23.4 μg mL^{-1}

Legend: MIC_{90}: minimal inhibitory concentration; CUR: curcumin; BNZ: benzydamine hydrochloride; $n = 3$.

This type of flow represents a pattern with distinct constant streamlines parallel to the direction of the fluid. Therefore, laminar flow allows the molecules within the fluid to be precisely manipulated, generating controllable monodisperse droplets, which represents the advantage of applying this type of synthesis for drugs encapsulation.[64] In a previous research performed by our group, with the aid of computational fluid dynamics, the velocity field and the flow pattern were calculated for this type of chip configuration and it was observed that as the Reynolds number increases the recirculation area (microvortex) also increases, improving the average mass transfer rates. The presence of the two microvortices indicates the rapid mixing of the inner and outer fluids, which is desirable for nanoparticle synthesis once it prevents the aggregation of material on the chip walls, preventing it from clogging.[65,66] The estimate mixing time is 0.67 s, which is in accordance with the literature since times smaller than 1 minute are desirable. The shorter the time, the more efficient the fluids mixing.[63,67]

2.3. In Vitro Synergism Assay (Checkerboard)

Although both drugs have antifungal activity, it is of paramount importance to predict the behavior of both drugs combined, in order to verify whether this association is desirable. Through calculations, a synergistic relationship between both drugs was observed, in addition, the drugs combination minimal inhibitory concentration (MIC_{90}) value was 19.5 μg mL^{-1} for CUR and

Table 2. Curcumin and benzydamine hydrochloride dual loading amounts and loading degree in the hybrid nanoparticle system.

System	CUR		BNZ	
	Loading amount [μg mL^{-1}]	LD%	Loading amount [μg mL^{-1}]	LD%
CUR@MSNs	158	16.3	–	–
BNZ@LP	–	–	69	6.7
CUR+BNZ@NIN	477	22	51	2.5

Legend: CUR: curcumin; BNZ: benzydamine hydrochloride; LD: loading degree; MSNs: mesoporous silica nanoparticles; LP: lipid bilayer of the NIN; NIN: hybrid nanoparticle; @: at $n = 3$.

23.4 μg mL^{-1} for BNZ (**Table 1**). In Figure S2 (Supporting Information) it is possible to observe the surface graph of all combinations.

2.4. Drugs Encapsulation

In addition to the loading degree (LD)%, **Table 2** shows the amount of each drug, in μg/mL, loaded into the particle based on the amount detected by high-performance liquid chromatography (HPLC). Highlighting this value is important once it allows a parallel with the amount of drug necessary to have the antifungal activity based on checkerboard results (Table 1). The fact that the incorporated value per mL is at least 1 time the combined MIC_{90} makes this a promising system.

2.5. In Vitro Drug Release

Figure 4A shows the release profile for both, free BNZ and BNZ loaded into NIN, around 60%. Despite being considered a water-soluble drug, the solubility of BNZ is not high, as reported elsewhere.[68] However, there is a consensus that it is better solubilized in ethanol than in water.[69–71] Another notable finding in the BNZ release profile is the increased release of this drug from NIN after a long plateau period. It is known that drugs already released can penetrate porous structures, so one possible hypothesis would be that the BNZ may have penetrated the MSNs and, as it has nitrogen in its structure, it could be linked with the silica matrix by hydrogen bonds. As proven by TEM, over time the silica matrix suffers erosion so, despite this time point was not analyzed by TEM, it can be suggested that around this time a more pronounced erosion happened, explaining this increase in the release.[72–74]

For CUR, it is possible to observe that its incorporation into the NIN increased the solubility of this drug, as a higher percentage of release was observed (50.3% in NIN and 31.5% for free drug), which is desirable since this drug is hydrophobic and the issue of its insolubility in aqueous solvent is a limiting factor for its application in therapy. It is worth highlighting that this not so high percentage of release is in line with previous studies in the literature.[75–77]

Figure 4B represents the triplicate DLS size reading of the three samples used for the release assay. It is possible to observe that the three samples showed the same pattern, being consistent with the release results, which shows a release plateau after 24 h (Figure 4A). It is worth mentioning that the measured size was higher than the NIN in deionized water one (Section 2.2) (Figure 4B), probably due to the simulated vaginal fluid content, which could have led to protein corona formation.[78,79]

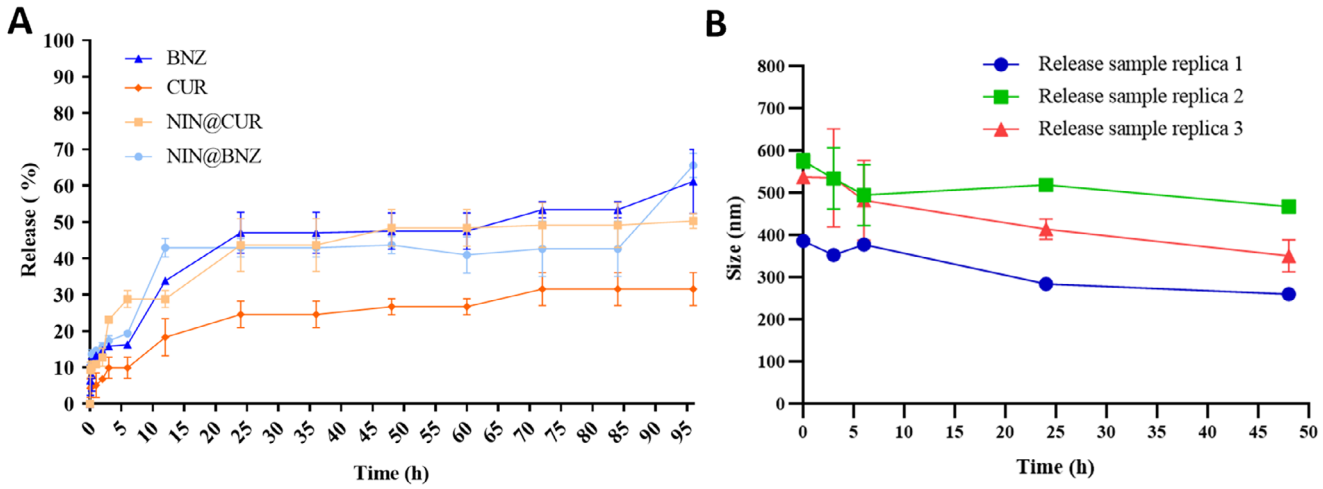

Figure 4. Results from the drug release tests of CUR and BNZ free drug combination compared to CUR+BNZ@NIN performed in simulated vaginal fluid under agitation at 150 rpm at 37 °C. Each experiment was performed in triplicate ($n = 3$) and the data are represented as the mean and the vertical lines represent the standard deviation of each value. A) Drug release profiles; B) The same release samples replicas were measure by DLS in order to observe the change in size during the experiment time. Legend: CUR: curcumin; BNZ: benzydamine hydrochloride; NIN: hybrid nanoparticle; @: at.

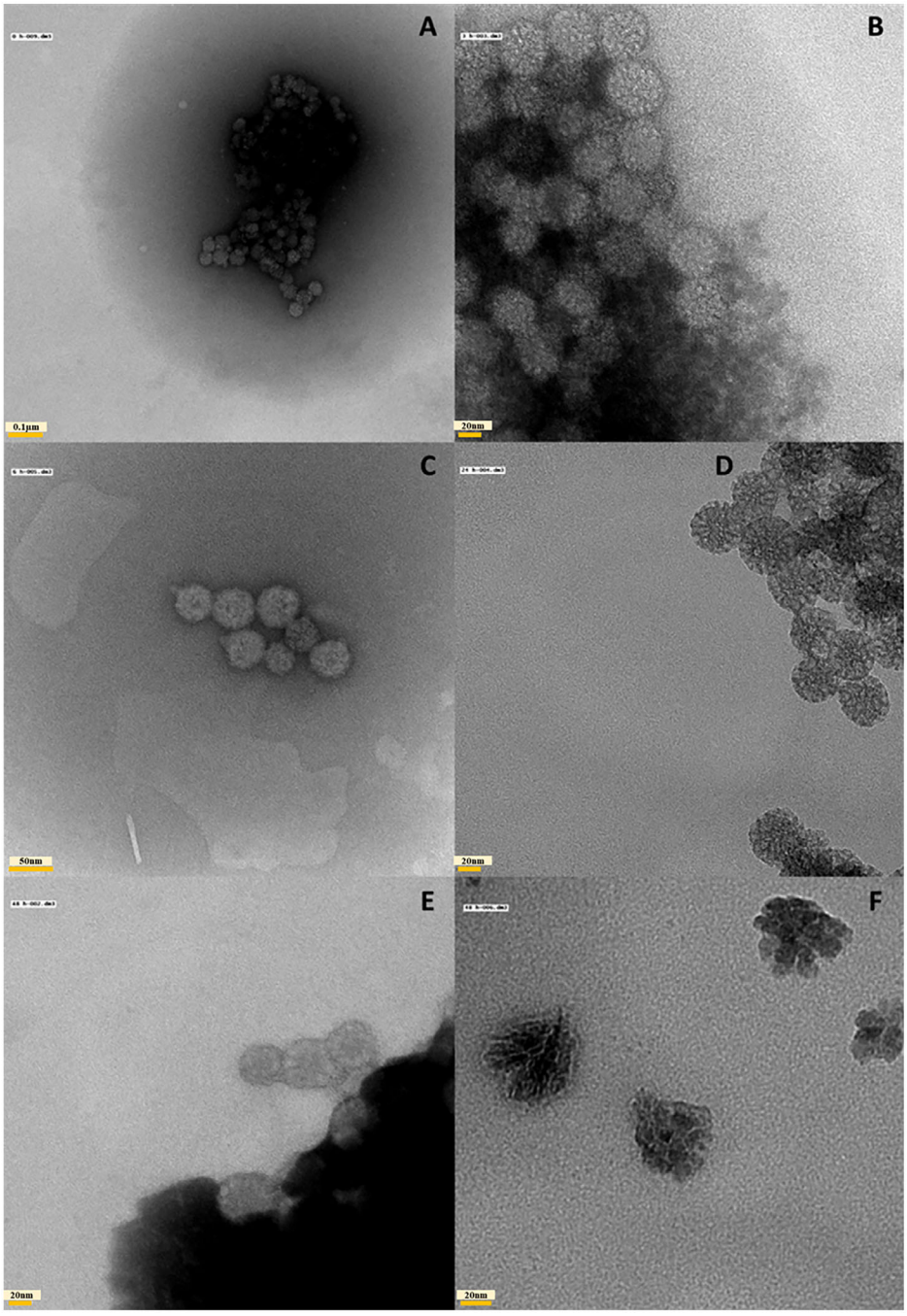

Figure 5. Representative transmission electron microscopy images of one release sample of some selected time points: A) at time 0 h – scale bar corresponds to 0.1 µm; B) 3 h – scale bar corresponds to 20 nm; C) 6 h – scale bar corresponds to 50 nm; D) 24 h – scale bar corresponds to 20 nm, and E, F) 48 h – both scale bars correspond to 20 nm.

Regarding the TEM of the samples collected during the drug release tests, it is possible to observe the formed NIN at time 0 (**Figure** 5A). However, at time 3 h (Figure 5B) they appear less stained at the edge (which indicates a smaller lipid bilayer). Additionally, at the edges of the aggregate it is possible to observe a morphology destruction, which may be caused by the lipid being destroyed. It is worth mentioning that black dots were observed (drug crystals). At 6 h (Figure 5C), it is difficult to observe the nanoparticle pores, which may indicate degradation, which seems to be more drastic at 24 and 48 h (Figure 5D–F)[36,80,81] This monitoring of NIN morphology carried out by TEM suggest that during the drug release tests, most likely, the lipid bilayer was disrupted, which enabled the drugs to be release from the nanohybrid. Moreover, the lipid disintegration and the MSNs

Table 3. Release kinetics mathematical models correlation coefficient value for curcumin and benzydamine hydrochloride combination as free drugs or incorporated in the hybrid nanoparticle.

Sample	Zero order	First order	Hixson Crowell	Higuchi	Korsmeyer-Peppas
Free BNZ	0.80	0.89	0.80	0.82	0.89
BNZ@NIN	0.84	0.91	0.84	0.89	0.91
Free CUR	0.81	0.91	0.81	0.89	0.91
CUR@NIN	0.85	0.89	0.85	0.91	0.89

Legend: CUR: curcumin; BNZ: benzydamine hydrochloride; NIN: hybrid nanoparticle; @: at.

degradation aspect over time in the simulated vaginal fluid point to their biodegradable behavior, which is desirable during the development of a new formulation.[82,83]

Regarding the mathematical models of release kinetics the correlation coefficient (R^2) value is used to select the model that best describe the release (the one closer to 1).[84] According to the results (**Table 3**), the first order was the most appropriate to explain BNZ release from BNZ at (@) NIN. The first order model describes drug release from a formulation as concentration-dependent, that is, the drug concentration decrease with the decrease in the concentration gradient over time.[85] The first order and Korsmeyer-Peppas were the most appropriate mathematical models to explain the release kinetics of free BNZ and CUR@NIN samples. Although Korsmeyer-Peppas R^2 for BNZ@NIN was also the highest number, it was not mentioned as the best model once this model is used for the first 60% of release which, in this case, was slightly higher.[86] Additionally, Korsmeyer-Peppas, also known as "power law", explains release as a semi-empirical method based on diffusion or swelling.[87] Higuchi was the mathematical model most appropriate to explain CUR release from NIN. The Higuchi model describes drug release as a time-dependent diffusion process based on Fick's law where the drug is released from an insoluble matrix once liquid molecules penetrates the system through the mesopores and slowly dissolves the drug into the acceptor media.[88,89]

2.6. Storage Stability Assessment

Stability assessment is an important tool during the development of a formulation as it predicts its behavior during storage. Regarding the size, no statistically difference was observed between times 0 and 30 days (**Figure 6A**). In the following times (from 45 days onwards), a statistically difference (p value < 0.0001) was observed when compared with time 0, suggesting loss of stability. It is worth noting that no statistically difference was observed for the other parameters. In view of the zeta potential result, we hypothesize that the stability loss after 30 days is due to the lipid nanoparticle layer disintegration; MSNs without this lipid bilayer has a highly negative zeta potential (−23.4 mV), but after its encapsulation by the lipids, a hybrid nanoparticle with zeta potential close to neutrality (−5.31 mV) was obtained, therefore, the MSNs that is losing the lipid layer would be more negative than the hybrid particle. For the purpose of confirming this issue, TEM analysis was carried out in the 60 day sample and as it can be seen in Figure 6B, the amount of NIN present is lower compared to Figure 3B, supporting the abovementioned hypothesis.

2.7. In Vitro Cytotoxicity Evaluation

Figure 7 shows that the four highest doses tested of the free drugs showed cytotoxicity for Normal Human Dermal Fibroblasts (NHDF) cells; however, when loaded into the NIN particles, no cytotoxicity was observed at any of the concentrations tested, demonstrating that the drug-loaded NIN system bypassed the cytotoxicity limitation of the drugs combination, which is desirable in terms of applying this formulation in therapy. Finally, Figure S3 shows how viability affects cell morphology during 48 h of incubation.

2.8. Evaluation of Antifungal Activity In Vitro

Although the Clinical & Laboratory Standards Institute (CLSI)[90] recommends 48 h of incubation, it was decided to also test an incubation time of 72 h to guarantee adequate time for antifungal activity, since the incorporated drug would have a barrier to overcome, meaning that the drug would have to first be released from the nanocarrier and then be available to carry out its activity. For the ATCC strain, it was observed that no formulation showed activity at the tested concentrations, neither at 48 h nor at 72 h. However, for the clinical strain, the highest concentration of CUR@MSN tested, 596.25 μg mL^{-1}, was MIC_{50} in 48 h. The other conditions tested showed no activity.

Even though CUR+BNZ@NIN did not show activity in this in vitro study, it was decided to continue the development of this formulation since although in vitro tests are used to predict the behavior of a formulation during its in vivo application, it is possible to observe in the literature that this is not always the case. For example, in a study whose objective was the development of a nanoemulsion containing micafungin against *C. auris* infection, it was observed that although free micafungin presented excellent activity (MIC_{90} of 0.062 mg mL^{-1}) when incorporated into the nanoemulsion no activity was observed in vitro. However, in the antifungal in vivo assay with *Galleria mellonella* it was observed that in addition to having extremely superior activity compared with the free drug (greater reduction in the counting forming units (CFU) number) the nanoemulsion incorporated with the drug was also able to completely eradicate the infection on the second day of treatment.[91] In a study performed elsewhere,[92] it was observed that lower doses of silver nanoparticles showed low percentages of fungal inhibition (less than 20%); however, in the in vivo test, a better activity was observed.

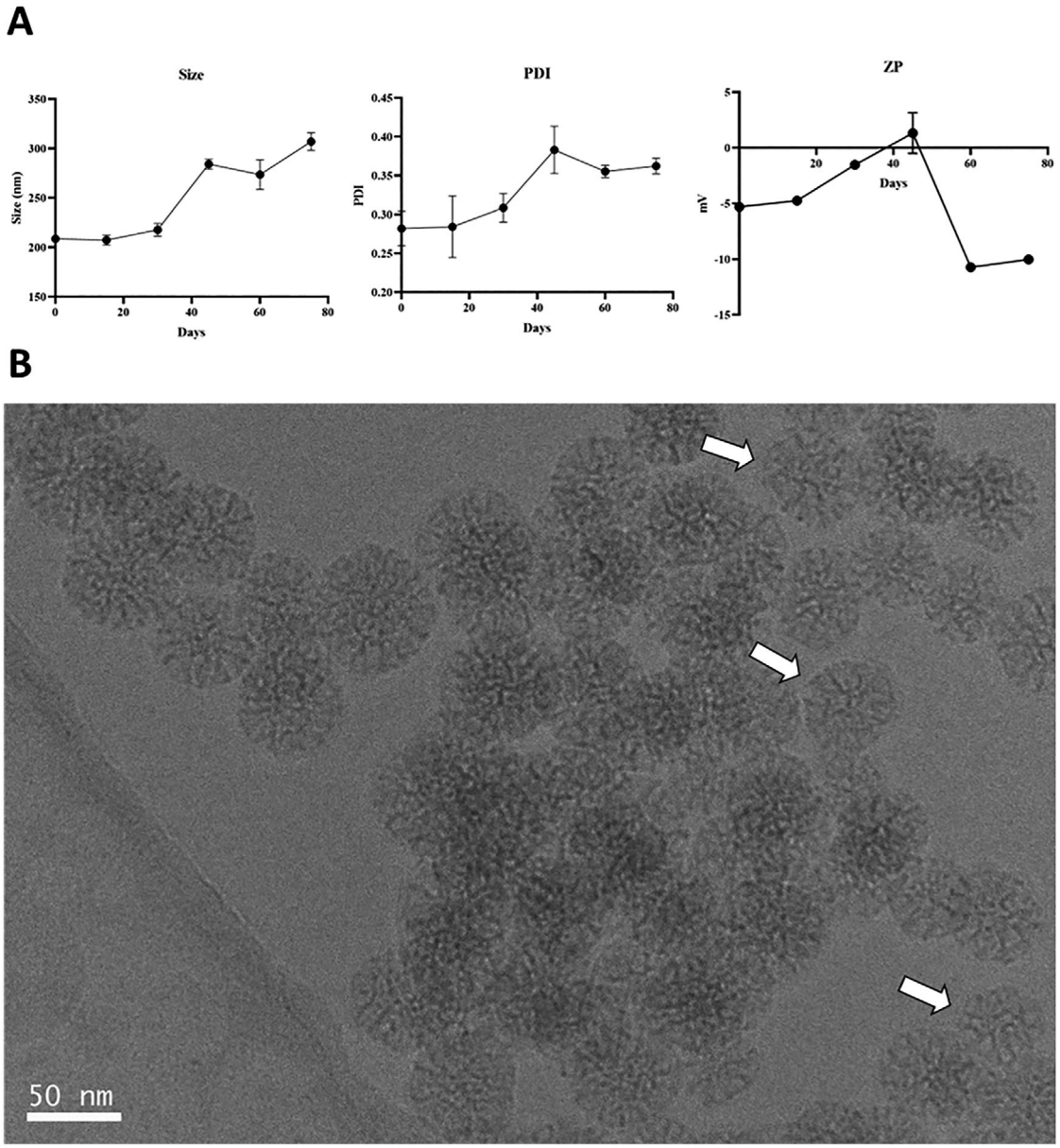

Figure 6. Stability of CUR+BNZ@NIN particles over time stored in a refrigerator A) tracking by dynamic light scattering for 75 days after synthesis, the data are represented as the mean of a triplicate ($n = 3$) and the vertical lines represent the standard deviation of each value. B) Representative transmission electron cryomicroscopy image after 60 days of synthesis (white arrows indicate the lipid-bilayer). Legend: CUR: curcumin; BNZ: benzydamine hydrochloride; NIN: hybrid nanoparticle; @: at; PDI: polydispersity index; ZP: zeta potential.

2.9. Thermo-Responsive and Mucoadhesive Hydrogel Containing CUR+BNZ@NIN Development, Characterization and In Vitro Drug Release Test

From the formulations developed, the best one contained 19% of poloxamer, since when associated with NIN it has a gelation point of ca. 33 °C (**Figure** 8A), within the range considered ideal for thermosensitive hydrogels for topical application (26 to 34 °C).[48,93] Without NIN, the observed gelation point decreases (Figure 8B), a behavior that has already been reported in the literature; however, the point of choice was based on the final formulation NIN@hydrogel(HG).[48] In Figure S4 it is possible to observe the gelation graph of the other attempts. According to the literature, to be considered viscous, a substance must have a viscosity greater than 1000 mPas.[94] In Figure 8C and D it is possible to observe that at temperatures of 30 °C and 25 °C, NIN@HG and the pure hydrogel, respectively, present this viscosity, which is in agreement with the gelation data.

In Figure 8E and F it is possible to observe the frequency sweep, it is worth noting that the lower angular frequencies observed indicates a solid-like substance. Additionally, the fact of the almost crossover observed in the NIN@HG graph indicates that it is stickier than the pure hydrogel, probably due to the fact that the temperature influences its viscosity.[95,96] Finally,

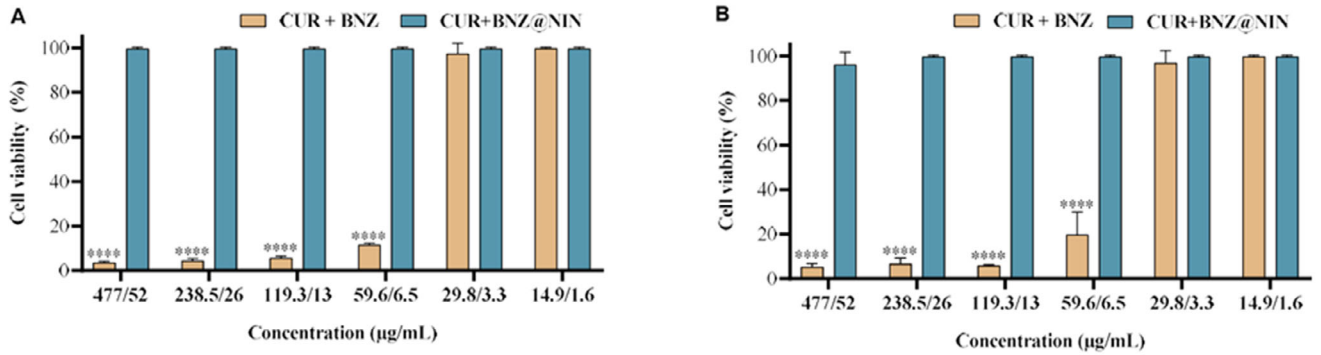

Figure 7. Cytotoxicity evaluation of CUR+BNZ versus CUR+BNZ@NIN in NHDF cells at 24 h A) and 48 h B), using the CellTiter-Glo™ assay. Concentrations of 477, 238.5, 119.3, 59.6, 29.8 and 14.9 μg/mL of CUR and 52, 26, 13, 6.5, 3.3 and 1.6 μg mL^{-1} of BNZ were analyzed of both samples. Each experiment was performed in triplicate ($n = 3$) and the data are represented as the mean were analyzed by two-way ANOVA (****$p < 0.0001$). Legend: CUR: curcumin; BNZ: benzydamine hydrochloride; NIN: hybrid nanoparticle; @: at; NHDF: Normal Human Dermal Fibroblasts; ANOVA: Analysis of Variance.

the linear viscoelastic region determination allowed an immediate distinction to be made between gels and entanglement networks, and it is possible to observe in Figure 8G and H that both presented this region up to 0.1%, as the storage modulus were drastically greater than loss modulus.[97] Regarding the injectability test carried out with vaginal applicators on a texture analyzer, it was observed that at both temperatures tested, 37 °C and 25 °C, the force required to inject is low, around 1 N for the free hydrogel and between 0 and 1 for NIN@HG.

After the physical characterization, in vitro drug release tests were carried out, and the drug release profiles obtained with the samples dispersed in hydrogel (**Figure 9**) were compared with those without the hydrogel (Figure 4A). It is possible to observe that CUR showed a similar pattern (once free drug dispersed in the hydrogel showed 48.2% of release and CUR incorporated in the NIN and dispersed in the hydrogel showed 52.85% of release). However, the solubility of the BNZ increased significantly in both samples, loaded and free. This may be due to the presence of poloxamer in the formulation. In a study of hydrogel formulations with poloxamer and chitosan containing BNZ, it was observed that the formulation containing only poloxamer was the one with the highest percentage of release (100% in 6 h), which is in accordance with what was observed in this study.[98] Other studies in the literature have also shown that after dispersion in hydrogels, BNZ shows 100% of release.[99] In another study, where two percentages of poloxamer were compared (18 and 20%), although not statistically different ($p > 0.05$), the authors also highlighted that the increase in poloxamer 407 concentration reflects an increase in BNZ release.[48] A possible hypothesis for this fact would be that the mixture of polymers present in the hydrogel can affect the crystallinity of this drug, increasing its solubility.[100]

Regarding the mathematical models of release kinetics, according to the results (**Table 4**), the zero order and Hixson Crowell was the most appropriate models to explain the release kinetics of BNZ and CUR@HG and BNZ@NIN@HG samples. The zero order model is related to a slow release of drugs from formulations that do not disaggregate.[101] The Hixson Crowell model correlates the initial drug mass present in the system with the drug mass remaining at time t, that is, the drug not released.[102] This model defines releases where changes in surface area occur, it is suitable for representing dissolution processes and may therefore represent the action of the hydrogel in the drugs release.[87] Finally, sample CUR@NIN@HG can be explained by the first order and Korsmeyer-Peppas models, both already discussed in section 2.5. However, it is worth highlighting that, according to the literature, the Korsmeyer-Peppas method can properly represent drug release from hydrogels.[87]

2.10. Antifungal and Anti-Inflammatory Activity Evaluation in In Vivo Mice Model

BALB/c mice were chosen as they have a better response to PMN cells, which have been shown to act directly to combat this type of fungal infection in humans.[103–105] To monitor the effect of the three doses administered to the animals in the statistical analysis the log CFU/mL value of each post-treatment sample was compared with the respective log CFU/mL value after infection (before starting the treatment) and it was observed that only the BNZ@NIN group did not show statistically differences (p value 0.0921), showing that this sample prevented fungal load to increase. In all other groups, this increase was statistically different (p value < 0.0001), except in the negative infection control group.

According to the candidiasis distribution in the vaginal epithelium, in histopathological analysis (main results summarized in **Table 5** and **Figure 10**A), it was observed that the combination of the two drugs was the most effective treatment in reducing the fungal amount, highlighting the potential of this combination for the treatment of this disease. Another factor that reinforces this observation is its greater efficiency compared to the commercial formulation. However, about the semi-quantitative candidiasis analysis (fungal burden) it is important to highlight that CUR@MSNs showed better results both in this parameter and in the in vitro study (Section 2.8). It was observed that CUR+BNZ@NIN, BNZ@NIN and the commercial formulation were the second-best treatment options, which indicates that they present similar therapeutic efficiencies. It is also important to highlight that in the groups treated with CUR+BNZ@HG, CUR

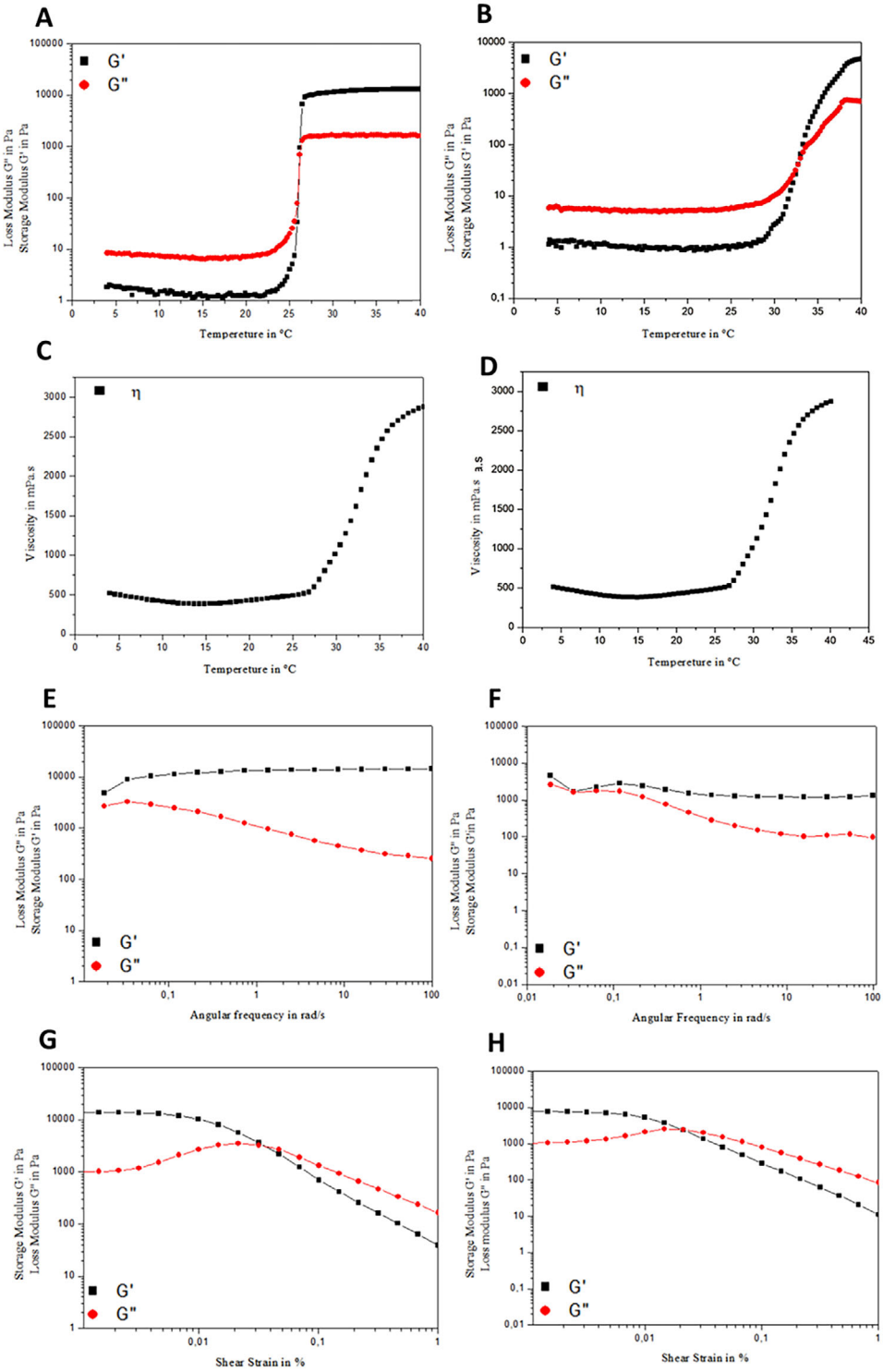

Figure 8. Rheology results of the prepared hydrogel ($n = 3$). A) Pure hydrogel gelation analysis; B) NIN@HG gelation analysis; C) Pure hydrogel viscosity versus temperature analysis; D) NIN@HG viscosity versus temperature analysis; E) Pure hydrogel frequency sweep analysis; F) NIN@HG frequency sweep analysis; G) Pure hydrogel linear viscoelastic range analysis; H) NIN@HG linear viscoelastic range analysis. Legend:NIN: hybrid nanoparticle; @: at; HG: hydrogel; G': storage modulus; G": loss modulus.

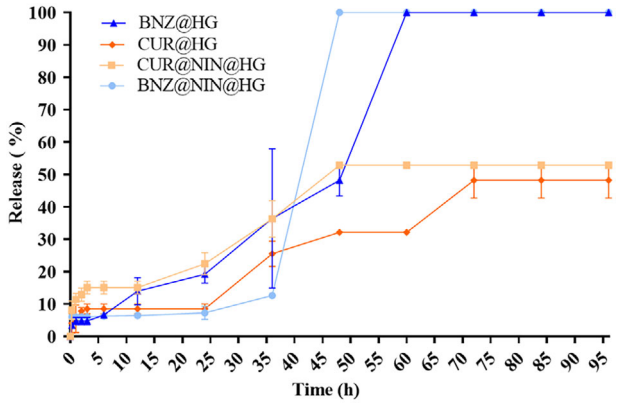

Figure 9. Release profile of CUR and BNZ from dual-loaded CUR+BNZ@NIN@HG compared to CUR+BNZ@HG in simulated vaginal fluid kept under agitation at 100 rpm at 37 °C. Each experiment was performed in triplicate ($n = 3$) and the data are represented as the mean and the vertical lines represent the standard deviation of each value. Legend: CUR: curcumin; BNZ: benzydamine hydrochloride; NIN: hybrid nanoparticle; HG: hydrogel; @: at.

and BNZ, a high increase in the scale points was observed, and in the case of BNZ, statistically difference (p value of 0.0203) was observed when compared with the infection control; showing that the incorporation of the drugs in the NIN increased their therapeutic potential. When incorporated in the hydrogel, the NIN nanosystem was not as effective as the non-incorporated one; however, the efficacy was still superior when compared to the free drugs groups (p value of >0.9999 in both cases).

One of the characteristic inflammation symptoms present in VVC is itching and redness (like in eczematous dermatitis), in histopathological analysis it reflects in epidermis infiltration with PMN cells characterizing spongiosis (Figure 10C and D).[106,107] In this study, the presence of infection, although not statistically different ($p = 0.050$), was shown to increase the amount of spongiosis (Table 5). When comparing the infection control group with other groups, it was observed that mice treated with CUR+BNZ@NIN@HG, CUR+BNZ@NIN, CUR+BNZ and commercial formulation showed, although not statistically different ($p = 0.9815$, 0.9815, 0.9998 and 0.8298, respectively), an expressive reduction in the spongiosis amount. This confirms the already well-established fact that the use of BNZ in the treatment of VVC is an interesting option. It is worth highlighting that it is common to observe residual inflammatory infiltrates in VVC treated groups in in vivo model.[108] In parallel, a correlation analysis was carried out between candidiasis-fungal burden and spongiosis parameters of each sample, and the CUR+BNZ@NIN

Table 4. Release kinetics mathematical models correlation coefficient value for free curcumin and benzydamine hydrochloride dispersed in the hydrogel and curcumin and benzydamine hydrochloride incorporated in the hybrid nanoparticle and dispersed in the hydrogel.

Sample	Zero order	First order	Hixson Crowell	Higuchi	Korsmeyer-Peppas
BNZ@HG	0.96	0.77	0.96	0.93	0.77
BNZ@NIN@HG	0.82	0.73	0.82	0.77	0.73
CUR@ HG	0.82	0.73	0.82	0.77	0.73
CUR@NIN@HG	0.86	0.93	0.86	0.92	0.93

Legend: CUR: curcumin; BNZ: benzydamine hydrochloride; NIN: hybrid nanoparticle; HG: hydrogel; @: at.

Table 5. Main results of the histopathological analysis performed with the vulva and vagina stained with periodic acid-Schiff. These values represent the average of an $n = 7$ animals per group (except group 9 where the values represent the average of an $n = 6$ animals).

Group	Parameter in scoring units			
	Candidiasis		Spongiosis	Sawtooth projections
	Distribution	Fungal burden		
Negative for infection	0.000	0.000	0.000	0.000
Positive for infection	1.285	1.428	1.142	0.714
CUR+BNZ@NIN@HG	1.166	1.500	0.666	0.571
CUR+BNZ@NIN	1.571	1.166	0.666	0.714
CUR+BNZ@HG	1.166	2.00	2.000	0.857
BNZ@NIN	0.857	1.166	2.000	0.714
CUR@MSNs	1.000	1.000	1.428	1.000
CUR+BNZ	0.666	1.142	0.857	0.571
CUR	1.000	2.000	1.333	1.000
BNZ	1.666	2.667	0.500	1.000
Commercial formulation	0.833	1.166	0.500	0.500

Legend: CUR: curcumin; BNZ: benzydamine hydrochloride; NIN: hybrid nanoparticle; HG: hydrogel; MSMs: mesoporous silica nanoparticles; @: at; commercial formulation: clotrimazole.

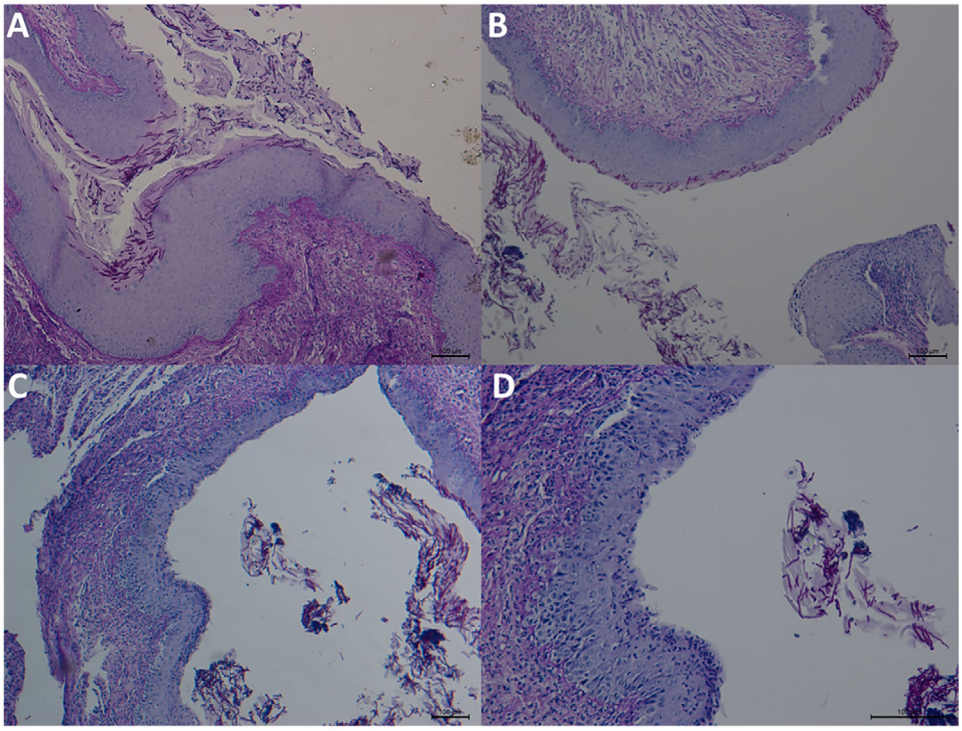

Figure 10. Representative histopathological sections of vulva and vagina stained with periodic acid-Schiff, all scale bars correspond to 100 µm A) Candidiasis and tissue desquamation with fungi; B) Epithelium with "sawtooth projections"; C) Spongiosis (20×); D) Spongiosis (40×).

group were the only treatment group that showed a statistically difference (p value of 0.0161), which indicates that the decrease in spongiosis observed in the CUR+BNZ@NIN group is directly connected to the decrease in fungal load in this same group. Another parameter that is worth highlighting is the sawtooth projections (Figure 10B), which is very common in histological findings of inflammatory diseases.[109–111] It is formed from a corrosive action of the inflammatory infiltrate on the epithelium, leading to disorganization of the basal layer.[109] These three parameters combined (fungal burden, spongiosis and sawtooth projections) suggest the therapeutic potential of CUR+BNZ@NIN@HG and its therapeutic equivalence with the commercial formulation.

The itching characteristic of VVC leads the patient to scratch or rub in the hope of relieving this uncomfortable symptom. However, this act can lead to tissue hyperkeratosis, which corresponds to keratinization of the affected area.[112,113] In this study, hyperkeratosis showed no statistically difference (p value of >0.9999), between the control groups; this can be attributed to the increase in keratinization observed with the complete resolution of the skin rash, considering a seven-day therapeutic regimen, this time may have been enough to improve symptoms and infection resolution, but not enough for mucosal keratinization.[114] Furthermore, the inflamed tissue may have lesions, which as they progress to chronicity, become thicker due to hyperplasia of the epithelium (acanthosis). This parameter is generally mild or absent when there is spongiosis or inflammation, probably this may be the reason why this parameter was not relevant for this study during data analysis (negative and positive control groups for infection presented very close values). It is worth highlighting that acanthosis generally occurs in areas with the presence of fungal hyphae and its occurrence is related to the clinical progression to vulvar carcinoma.[115–118] Finally, atrophy is a common histopathological finding during VVC as it is a consequence of the decrease in estrogen levels.[119] However, in this study, changes in this parameter were unremarkable probable due to the estradiol doses administered during the trial, a key step for the establishment of vaginal infection in vivo.[120,121]

Finally, it is worth mentioning that during this experiment there was only the death of one animal in group 9 (treated with free curcumin), this fact occurred on the 22nd day of the experiment.

3. Conclusion

In this study, we reported the development of a hybrid nanoparticle dual-loaded with CUR and BNZ to combat not only the *Candida* infection but also to relieve the inflammation symptoms caused by the invasion of this fungus' pseudohyphae in the vaginal mucosa. In order to develop a hybrid nanoparticle composed by MSN inside a liposome in a reproducible manufacturing way a new microfluidics approach was optimized as an innovative and efficient solution. Through in vitro cytotoxicity studies, it was possible to determine that in addition to being safe, the drugs-loading in the nanoparticle drastically reduced their toxicity. In addition, despite the checkerboard microdilution assay pointed to how promising the antifungal activity of these drugs combination is against resistant *Candida albicans* strains, after the loading in the hybrid nanoparticle no activity was observed in vitro.

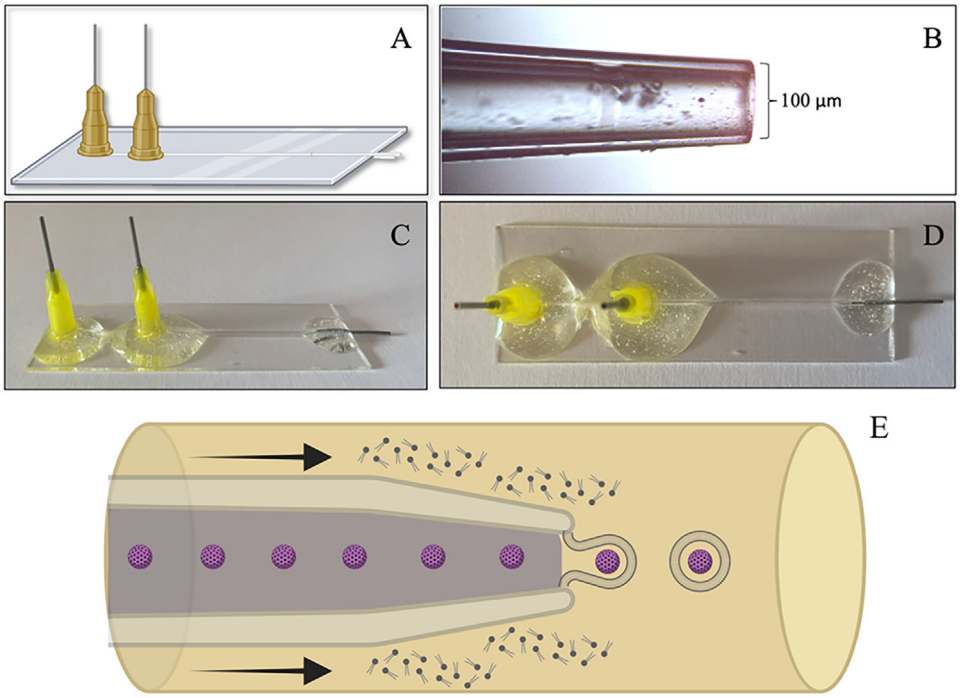

Figure 11. Microfluidics microchip used for the hybrid nanoparticle synthesis. A) Graphic representation; B) Microscope image of the inner capillary with 100 µm diameter; C) Side view of the microfluidics chip; D) Top view of the microfluidics chip; E) Schematic hypothesis of the hybrid nanoparticle system assembly by the co-flow microfluidics system. The hybrid nanoparticle consists of CUR-loaded MSN encapsulated into a BNZ-loaded lipid-bilayer. Legend: CUR: curcumin; BNZ: benzydamine hydrochloride; MSN: mesoporous silica nanoparticle.

However, the histology performed in the in vivo study pointed to CUR+BNZ@NIN antifungal and anti-inflammatory therapeutic potential. Ultimately, this study offers new possibilities for the development of silica-based hybrid nanoparticles by microfluidics and at the same time highlights the potential combination of CUR and BNZ for the treatment of VVC.

4. Experimental Section

Mesoporous Silica Nanoparticles Synthesis and Characterization: MSNs were synthesized according to Carvalho et al.[54] with some modifications. First, 0.61 g of cetyltrimethylammonium bromide (CTAB) (Sigma-Aldrich) and 180 mL of distilled water were added in a round bottom flask and kept under stirring at 60 °C for 30 min. Then, 55.8 mL of octane (Fisher Scientific), 105 µL of styrene (Fisher Scientific) (previously washed three times with 2.5 M NaOH), 0.14 g of L-Lysine (Fisher Scientific), 6.42 mL of tetraethyl orthosilicate (TEOS) (Sigma-Aldrich), 0.20 g of sodium dihydrochloride 2,2′- Azobis (2-methylproprylnamide) (AIBA) (Fisher Scientific), were added. After, with the help of a needle, nitrogen was immersed in the mixture for approximately 30 min, then the needle was lifted but kept inside the flask throughout the reaction time (3 h). It is worth noting that during this period the magnetic stirring and the temperature of 60 °C were maintained.

After, the suspension was transferred to a separatory funnel for phase separation overnight (room temperature). Then, the suspension phase was collected and centrifuged (Sorvall Discovery 90SE, Kendro Laboratory Products) at 21,000 rpm for 15 min, the precipitate was washed 5 times with distilled water and ethanol. At the end of the washes, the precipitate was suspended in 60 mL of methanol. Sequentially, the particles were subjected to an acid reflux step, for this 15 mL of chloroform and 1.5 mL of hydrochloric acid were added and kept under reflux with magnetic stirring at 60 °C for a period of 6 h. Then, the resultant solution was centrifuged at 21,000 rpm for 15 min, the precipitate was washed 5 times with distilled water and ethanol.[54] Last, the precipitate was dispersed in 4-(2-hydroxyethyl)−1-piperazineethanesulfonic acid (Hepes buffer) (pH 7.4) (Sigma-Aldrich) and kept under refrigeration (1 °C – 4 °C).

In order to evaluate the MSNs formation hydrodynamic size, PDI and zeta potential were evaluated by DLS (ZEN3600, Malvern Panalytical Ltd.,) using Hepes buffer (pH 7.4) as the dispersant. Additionally, FTIR Golden Gate Single Reflection Diamond attenuated total reflectance (ATR) System (AgilentTechnologies Cary 670 and sliding wear tester TR-17), TG (PerkinElmer TGA-7) (using a synthetic air purge; measure program done stepwise using 10 °C min^{-1} heating ramp with 25 min isothermal segments at 35 °C and 120 °C) and nitrogen sorption analysis (at 196 °C in a Micromeritics 3Flex 3500) using the BET method to calculate the surface area. Pore volume was estimated as the total adsorbed amount at a relative pressure of $p/p_0 = 0.97$ while pore size distribution was calculated with MicroActive v5.01 software (Micromeritics Corp.) using density functional theory, assuming cylindrical pores with kernel model for oxide surfaces. Prior analysis the sample was degassed at 120 °C under high vacuum. Finally, TEM (TalosF200i operating at 80 KeV with a Ceta 16 M camara) was also carried out.

Preparation and Characterization of the Hybrid System: A cylindrical borosilicate glass capillary (WPI) (external diameter of 1000 µm) was tapered at one of its ends with the aid of a micropipette puller (P-1000 Sutter Instrument). Then it was polished until an internal diameter of 100 µm.[122–124] It was then inserted into a cylindrical borosilicate glass capillary, (internal diameter of 1.1 mm). Dispensing needles (McMaster-carr) were fixed at the beginning of each capillary to facilitate the entry of inner and outer fluids (**Figure 11**A–D). The inner fluid was composed of MSNs (2 mg mL^{-1}) and the outer fluid composed by egg yolk phosphatidylcholine (E80 ©Lipoid) and soybean phosphatidylcholine (S100 ©Lipoid) solubilized in ethanol (10 mg mL^{-1} each). It is worth noting that the microfluidics system consisted of two syringe pumps (PHD

Ultra Harvard Apparatus) and a microscope (Leica DM IL LED).[125–127] Regarding the flow, several attempts were made (1:7; 1:10; 1:5; 1:2.5; 9:1; 7:1).[124,128] It is worth mentioning that the samples were collected in a solution containing 1% poloxamer in deionized water. Formulations with a PDI close to or below 0.2 in DLS analyses (using deionized water as the dispersant) were further characterized by TEM. Additionally, to confirm the formation of the hybrid nanoparticle Cryo-TEM (Tecnai T20 – FEI, Eindhoven the Netherlands with an Us400 slow scan CCD camara and operating at 200 keV) and EDX (X-max 80T SDD detector, Oxford instruments) analyzes were performed.

In order to better understand the chosen synthesis condition, numerical analyzes were carried out. First, to confirm the laminar flow, the Reynolds number was calculated according to Equations 1–3. Equation 4 was used to estimate the mixing time:[62]

$$\text{Reynolds number} = \frac{\rho \text{UL}}{\mu} \tag{1}$$

where, ρ was the fluid density, U the average fluids velocity, L the hydraulic diameter and μ the fluid viscosity. Equations 2 and 3 were used to calculate U and L respectively.

$$\text{U} = \frac{\text{Flow rate}}{\text{W.H}} \tag{2}$$

where, W was the width and H the height of the channel.

$$\text{L} = \frac{4\,\text{W.H}}{\text{Pwet}} \tag{3}$$

Where, Pwet was the wetted perimeter.

$$\tau_{\text{mix}} = \frac{wf^2}{4D} \tag{4}$$

where, wf was the inner stream width and D the solvent diffusion constant.

In Vitro Synergism Assay (Checkerboard): Figure S5 describes this methodology in detail. Briefly, for this assay, two 96-well microplates were used. One of them with CUR (Pharmaceutical Secondary Standard from Supelco) in the concentration range of 1000–7.8125 µg mL^{-1}, and the other with BNZ (analytical standard from Sigma-Aldrich) in the concentration range of 1000–12.625 µg mL^{-1}. Concentration of 1×10^3 yeasts/mL of *C. albicans* FMB-01 (clinical strain resistant to azoles provided by the Medical School of São Paulo State University; Ethical Assessment: 55 758 222.6.0000.5411) was used as the inoculum. The results were analyzed according to the fractional inhibitory concentration index (FICI), if FICI ≤ 0.5 the drugs combination have a synergism effect, if FICI in the range of > 0.5 – < 4.0 the drugs combination has a neutral effect and if FICI > 4.0 the drugs combination has an antagonistic effect.[90,129]

Drugs Encapsulation: Prior to the drug encapsulation stage in the hybrid nanoparticle system, there was a need to develop and validate an HPLC (Agilent, 1260 infinity II) analytical method with a C18 column (Sulpelco 15 cm × 4.6 mm, 5 µm) in order to allow the separation and detection of both drugs, CUR and BNZ. Regarding the development of the HPLC method, the best condition observed was the gradient of 70:30 acetonitrile and 0.2% phosphoric acid in water 0.9 mL mi^{-1}n over 1.5 min, change in the flow to 1.5 mL mi^{-1}n over 0.5 min and change of the mobile phase composition to 80:20. The best detection wavelength was 230 nm.[13,130] In Figure S6 it is possible to observe the HPLC chromatogram, the first peak corresponds to the BNZ and the second corresponds to CUR.

After, the drugs were encapsulated. Firstly, CUR was loaded into MSNs, and for this, 2.5 mg mL^{-1} of the drug was dissolved in 750 µL of ethanol and kept stirring at 8 °C. Next, 250 µL of MSNs (20 mg mL^{-1} in Hepes buffer) was added, and the solution was kept shaking for 24 h. Then, the nanoparticles were collected, centrifuged at 14 000 rpm for 15 min and the precipitate was resuspended in a basic ethanolic solution and maintained under magnetic stirring for 24 h to destroy the MSNs. After this period, it was centrifuged under the same conditions mentioned above and the supernatant was read in HPLC.

For BNZ encapsulation into the lipid bilayer, 1 mg mL^{-1} of the drug was dissolved in an ethanolic solution containing the lipids, then the hybrid nanoparticle system was synthesized as described in Section *"Preparation and Characterization of the Hybrid System"*. To evaluate the amount of incorporated drug, 1 mL of NIN was centrifuged (Eppendorf 5417r) at 3000 rpm for 5 min and the precipitate was resuspended in 500 µL of chloroform in order to destroy the lipid bilayer of the particle. The solution was filtered and analyzed in HPLC. Finally, after evaluating the amount of drug incorporated separately, the simultaneous incorporation was evaluated, and for this, immediately after CUR encapsulation in the MSNs the NIN was prepared with the other drug, and the quantification of both drugs encapsulation was performed in both methods mentioned above. The LD% was calculated according to Martins et al.[82] The hybrid nanoparticle system formation after the drugs' encapsulation was evaluated by both TEM and Cryo-TEM.

In Vitro Drug Release: To have a preview of the developed nanosystem behavior, a preliminary release study was performed on a shaker incubator equipment, which allowed the samples (CUR+BNZ@NIN and CUR+BNZ, in triplicate) to remain at 37 ± 0.5 °C under constant stirring of 150 rpm during the entire assay.[17] For this study, the sink conditions were respected.[131] To mimic the vaginal environment, the acceptor medium contained simulated vaginal fluid (Biochemazone), 2% tween 80 and 5% propanol, with a pH of 4.5, compatible with the human vaginal one.[131,132] Samples aliquots (200 µL) were collected at multiple times points (10 min; 30 min; 1 h; 2 h; 3 h; 6 h; 12 h; 24 h, 36 h, 48 h, 60 h, 72 h 84 h and 96 h), additionally, at each collection point the same volume of acceptor medium was replaced. The drug content in the aliquots was quantified by the validated HPLC method, as described above. Additionally, the samples collected at times 0, 3 h, 6 h, 24 h e 48 h were evaluated for its size by DLS and morphology by TEM (CM12, Philips Eindhoven, operating at 120 keV with an Us400 slow scan CCD camara). For the TEM the samples were negatively stained with phosphotungstic acid (PTA) 1% in water.[124] Different mathematical models were applied to analyze the release kinetics of CUR and BZH incorporated in the hybrid nanoparticle. The release results were analyzed following zero order (Equation 5), first order (Equation. 6), Hixson Crowell (Equation. 7), Higuchi (Equation. 8) and Korsmeyer-Peppas (Equation. 9) calculations.[133,134]

$$\frac{M_t}{M_\infty} = \text{K}_0\text{t} \tag{5}$$

$$\frac{M_t}{M_\infty} = 1 - e^{-\text{K1t}} \tag{6}$$

$$Q_{0_3}^1 - Q_3^1 = \text{K}_{\text{HC}}\text{t} \tag{7}$$

$$\frac{M_t}{M_\infty} = \text{K}_\text{H} t_2^1 \tag{8}$$

$$\frac{M_t}{M_\infty} = \text{K}_{\text{KP}} t^n \tag{9}$$

where, M_t was the amount of drug released at time t; M_∞ the amount of drug released after infinite time; K_0 was the release rate constant for zero-order; K_1 the release rate constant for first-order; K_H the release rate constant for Higuchi diffusion; Q was the residual drug % in the matrix at time t; K_{HC} was the Hixson-Crowell constant; K_{KP} was a constant related to the dosage form structural and geometric characteristics; n was the release exponent.

Storage Stability Assessment: In order to determine the time range that a formulation will still be adequate for use in the laboratory and also to make a correlation with its shelf-life, samples were prepared (day 0) and analyzed by DLS regarding its size, PDI and zeta potential. The samples were then stored in a refrigerator and analyzed every 15 days. It was worth

noting that shortly before DLS analysis, the samples were centrifuged at 3000 rpm for 5 min and the precipitate was resuspended in 1 mL of deionized water. Finally, using Cryo-TEM, at a time point of choice that they were not stable, the difference in the nanosystem morphology was evaluated.

In Vitro Cytotoxicity Evaluation: NHDF were maintained in culture in Dulbecco's Modified Eagle's Media (high glucose) (Gibco) containing 10% fetal bovine serum and 1% Pen-Strep (Gibco).[135,136] Prior to the test, the cells were harvested with trypsin-ethylenediaminetetraacetic acid (EDTA)-phosphate buffer solution (Gibco) and diluted at a density of 1.5×10^5 cells mL^{-1}. Then, the cells were seeded in a 96-well (0.2 mL per well) and left to attach for 24 h. After the attachment, the medium was discarded, and the cells were washed with 200 µL of phosphate Buffer (PBS) pH 7.4. Next, the cells were exposed to the controls (9% Triton X-100 solution (Boom) as positive control and cell media as negative control), CUR+BNZ@NIN (concentration range 1–0.031 mg mL^{-1}) and free drugs (in concentrations corresponding to the drug amount present in the formulation dilutions, for CUR and BNZ respectively: 477–14.9 µg mL^{-1} and 52–1.6 µg mL^{-1}). Then, the plate was incubated for 24 and 48 h at 37 °C in 5% of CO_2 and 95% relative humidity. In order to quantify the number of viable cells CellTiter-Glo (© Promega corporation) assay was performed. The experiment was performed in triplicate.[137–139]

Evaluation of Antifungal Activity in Vitro: For the determination of the CUR+BNZ@NIN MIC two *C. albicans* strains were used, ATCC 18 804 and FMB-01. In addition to the main nanosystem, CUR@MSNs, BNZ@NIN and NIN (without drug) were also analyzed as controls. Since all formulations had the same amount of the respective drug present, the CUR and BNZ range evaluated was 596.25–4.65 µg mL^{-1} and 63.75–0.5 µg mL^{-1}. Prior the test, both strains were cultivated in 2 mL of sabouraud dextrose broth (SDB) (Difco-Becton) and incubated at 37 °C for 48 h, then, a suspension corresponding to 0.5 on the McFarland scale, and confirmed by cells count in a Neubauer chamber (*ca*. 1×10^6 cells mL^{-1}), were prepared. In order to have a inoculum with 5.0×10^3 cells mL^{-1} two consecutive dilutions were made (1:100 and 1:20).[90]

After, in a 96-well microplate 100 µL of Roswell Park Memorial Institute (RPMI 1640) medium with pH 7.0–7.2) was added in each well. The samples were added in the first-row wells and a serial dilution in the 8 subsequent wells were performed. Then, 100 µL of the inoculum were also added. It is worth mentioning that sterility and growth controls were also performed.[90] The microplate was incubated at 37 °C for 48 h. Finally, 20 µL of 2% triphenyltetrazolium chloride (TTC) (Sigma-Aldrich) solution was added and after an incubation of 2 h at 37 °C a visual reading was performed (lack of fungi growth remain colorless and growth turn the solution pink).

Thermo-Responsive and Mucoadhesive Hydrogel Containing CUR+BNZ@NIN Development, Characterization and In Vitro Release Test: Chitosan (1%) (Sigma-Aldrich) and poloxamer 407 (Sigma-Aldrich) were used to confer mucoadhesive and thermo-responsive characteristics, respectively, to the hydrogel.[46,140] Various poloxamer percentages were tested (15, 16.5, 17, 18, 19, 20, 25%) with the same manufacturing methodology. Initially, deionized water with 1% acetic acid was kept under magnetic stirring in an ice bath for 2 min. Then, chitosan was added and kept in magnetic stirring for another 40 min. After obtaining a homogeneous viscous substance, poloxamer was added gradually under magnetic stirring with the aid of manual stirring until a homogeneous solution was obtained. Subsequently, it was kept overnight in an ice bath.[141] To manufacture the hydrogel containing the nanosystem (CUR+BNZ@NIN@HG), a volume of 5 mL of CUR+BNZ@NIN was centrifuged at 3000 rpm for 5 min and then the precipitate was resuspended with 1 mL of hydrogel. A rheometer (Anton Paar MCR 92) was used to characterize the hydrogel with and without the nanosystem concerning its gelation point, viscosity versus temperature, frequency sweep (at 37 °C) and linear viscoelastic range (at 37 °C).[142–144] Additionally, a texture analyzer (Brookfield CT3) was used to evaluate the injectability of the final hydrogel (with and without CUR+BNZ@NIN) with the aid of a vaginal applicator, temperatures of 25 and 37 °C were tested.[142,144]

For the in vitro release test, some changes to the methodology carried out in Section *"In Vitro Drug Release"* were made. The experiment was performed in a 12-well microplate, while the acceptor media was added to the microplate well, the sample was added to cell culture inserts. The stirring speed was changed to 100 rpm. The samples analyzed were the NIN@hydrogel containing both drugs and the hydrogel with the combination of both free drugs. The same mathematical models used to analyze the release kinetics in Section *"In Vitro Drug Release"* were also applied here.

Antifungal and Anti-Inflammatory Activity Evaluation in In Vivo Mice Model: Female BALB/c mice with 8 to 10 weeks weighing around 20 to 25 g were used to this experiment. The animals were kept in cages at appropriate temperature, with ventilation, 12-h light/dark cycle with water and food available. In order to assist in the induction of the disease, the mice received 0.1 mL of estradiol solution (2 mg day^{-1}) intraperitoneally twice in week two.[120,121] Vaginal infection was induced by intravaginal application of 20 µL of a *C. albicans* suspension containing 2.5×10^8 cells/mL. In the post-infection period, doses of estradiol (Sigma–Aldrich) (alternate days) were administered (also intraperitoneally) to maintain the pseudoestrus state. In order to evaluate the formulation antifungal activity, vaginal washes were carried out with PBS 6 h before treatment, part of the collected volume was sown in sabouraud dextrose agar (SDA) with chloramphenicol (Difco-Becton). The plates were incubated at 37 ± 0.5 °C for 48 h, and the colony count was expressed in CFU/mL. The experimental protocol design, summarized in Figure S7 had a total treatment period of seven days.[17,145] It is worth highlighting that the experimental groups for the in vivo were carefully selected to obtain the smallest number of groups that included all the necessary comparisons (Table S1), with the smallest number of animals (sample calculation carried out in the software "Power & Sample Size Calculator").

As for dosage, 25 µg of BNZ (1 time the combined MIC_{90} value) and 239 µg of CUR (12 times the combined MIC_{90} value) were administered per application. It is worth noting that all formulations were applied at the same dosage, adjusting the final volume in order to standardize the same drug concentration. For the commercial formulation, Clotrimazole (Medley), one of the recommended medications by the Center of Disease Control and Prevention (CDC) for VVC treatment, was the one of choice.[146] The recommendation in the medicine leaflet was followed, adjusting dosage according to the animal's weight.

Immediately after the euthanasia, the animals were shaved in the vaginal region and through a longitudinal cut in the infra-abdominal region, the vulva and vagina of all animals were collected (and preserved in 4% formaldehyde for 7 days) for histopathological analysis. After this period, a macroscopic analysis was performed to identify the anatomical parts, which were sectioned longitudinally and included in paraffin. After, 4 µM sections were obtained, stained in periodic acid-Schiff and blindly evaluated by an experienced pathologist, previously calibrated. The analyses were performed at two different times with a minimum interval of 1 week between them. Light microscope (Carl Zeiss, Primo Star, Germany) was used at 100, 200, and × 400 magnifications.

Candidiasis was analyzed in two ways, first distribution classification as absent (0); focal (1), multifocal (2) and diffuse (3) and evaluated semi-quantitatively (fungal burden) in the absence of fungi (0), up to 5 fungal elements per section (standard: 5 mm punch) (1), from 6 fungal elements per section to 5 per field at high magnification (×400) (2), from 6 to 50 per field at high magnification (3) and more than 50 per field at high magnification (4).[147] In addition, other parameters were evaluated, such as spongiosis (absent (0), focal (1), multifocal (2) and diffuse (3)), and presence (1) and absence (0) of atrophy, acanthosis, hyperkeratosis and sawtooth projections. This in vivo experiment was approved by the School of Pharmaceutical Sciences of São Paulo State University; Ethical accreditation number: 02.00082.2019.

Statistical Tests: All statistical analyzes performed in this study were carried out in the software GraphPad Prism. For the Storage stability assessment two-way Analysis of Variance (ANOVA) with Tukey's multiple comparisons were carried out in order to determine significant changes in the evaluated parameters. Two-way ANOVA with Sidak's multiple comparisons was used to analyze the cytotoxicity results. To monitor the comparison of the log CFU/mL of each post-treatment sample with the respective log CFU/mL value after infection (before starting the treatment) Two-way

ANOVA with Dunnett's multiple comparisons was used, and to analyze the histology findings Two-way ANOVA with Tukey's multiple comparisons test were performed.

Supporting Information

Supporting Information is available from the Wiley Online Library or from the author.

Acknowledgements

The authors acknowledge São Paulo Research Foundation (FAPESP- grant numbers: 22/02187-0, 19/26821-7 and 19/09831-9), and UMCG Research Funds for the financial support.

Conflict of Interest

The authors declare no conflict of interest.

Data Availability Statement

The data that support the findings of this study are available from the corresponding author upon reasonable request.

Keywords

benzydamine hydrochloride, curcumin, lipids, mesoporous silica nanoparticles, thermo-responsive hydrogel, vulvovaginal candidiasis

Received: August 27, 2024
Published online:

[1] G. C. Carvalho, R. A. P. de Oliveira, V. H. S. Araujo, R. M. Sábio, L. R. de Carvalho, T. M. Bauab, I. Corrêa, M. Chorilli, *Med. Mycol.* **2021**, *59*, 946.
[2] M. F. Mushi, R. Olum, F. Bongomin, *Med. Mycol.* **2022**, *60*, myac037.
[3] G. G. G. Donders, K. Ruban, F. Donders, R. Reybrouck, *J. Clin. Med.* **2022**, *11*, 574.
[4] V. H. S. Araujo, J. L. Duarte, G. C. Carvalho, A. L. P. Silvestre, B. Fonseca-Santos, G. D. Marena, T. de C. Ribeiro, M. A. dos Santos Ramos, T. M. Bauab, M. Chorilli, *Crit. Rev. Microbiol.* **2020**, *46*, 508.
[5] W. J. Jane, J. S. Iramiot, J. B. Kalule, *Microbiol. Res. J. Int.* **2019**, *28*, 1.
[6] L. S. Barbedo, *DST J. Bras. Doenças Sex Transm.* **2010**, *22*, 22.
[7] D. Marchaim, L. Lemanek, S. Bheemreddy, K. S. Kaye, J. D. Sobel, *Obstet. Gynecol.* **2012**, *120*, 1407.
[8] F. Martins, D. L. Morgado, B. Sarmento, E. R. de Camargo, J. das Neves, *Int. J. Pharm.* **2023**, *647*, 123508.
[9] Y. K. Hsin, T. Thangarajoo, H. Choudhury, M. Pandey, L. W. Meng, B. Gorain, *J. Pharm. Sci.* **2023**, *112*, 562.
[10] A. J. Sucher, A. Thai, C. Tran, N. Mantena, A. Noronha, E. B. Chahine, *Am. J. Heal. Pharm.* **2022**, *79*, 2208.
[11] N. Hassan, S. Firdaus, S. Padhi, A. Ali, Z. Iqbal, *Med. Hypotheses* **2021**, *148*, 110515.
[12] C. Santezi, B. D. Reina, S. R. de Annunzio, G. Calixto, M. Chorilli, L. N. Dovigo, *Photodiagnosis Photodyn. Ther.* **2021**, *35*, 102416.
[13] G. Molinaro, F. Fontana, R. Pareja Tello, S. Wang, S. López Cérda, G. Torrieri, A. Correia, E. Waris, J. T. Hirvonen, G. Barreto, H. A. Santos, *ACS Appl. Mater. Interfaces* **2023**, *15*, 23012.
[14] M. A. Obeid, M. Alsaadi, A. A. Aljabali, *J. Liposome Res.* **2023**, *33*, 53.
[15] M. Cacaci, D. Squitieri, V. Palmieri, R. Torelli, G. Perini, M. Campolo, M. Di Vito, M. Papi, B. Posteraro, M. Sanguinetti, F. Bugli, *Pharmaceuticals* **2023**, *16*, 275.
[16] L. B. Pozharani, E. Baloglu, K. Suer, E. Guler, E. V. Burgaz, I. Kunter, *J. Drug Deliv. Sci. Technol.* **2023**, *86*, 104739.
[17] C. F. Rodero, G. M. Fioramonti Calixto, K. dos Santos, M. R. Sato, M. dos Santos Ramos, M. S. Miró, E. Rodríguez, C. Vigezzi, T. M. Bauab, C. E. Sotomayor, *Mol. Pharmaceutics* **2018**, *15*, 4491.
[18] J. Shi, M. L. Maguer, *Crit. Rev. Food Sci. Nutr.* **2000**, *40*, 1.
[19] R. Carolina Alves, R. Perosa Fernandes, B. Fonseca-Santos, F. Damiani Victorelli, M. Chorilli, *Crit. Rev. Anal. Chem.* **2019**, *49*, 138.
[20] G. C. Carvalho, R. M. Sábio, M. Chorilli, *Crit. Rev. Anal. Chem.* **2020**, *51*, 674.
[21] L. C. de Lima, M. A. S. Ramos, L. G. de Toledo, C. F. Rodero, F. Hilário, L. C. dos Santos, M. Chorilli, T. M. Bauab, *Curr. Pharm. Des.* **2020**, *26*, 1556.
[22] R. dos Santos, M. Aparecido, P. B. da Silva, L. G. de Toledo, F. B. Oda, I. C. da Silva, L. C. dos Santos, A. G. dos Santos, M. T. G. de Almeida, F. R. Pavan, *J. Biomed. Nanotechnol.* **2019**, *15*, 1072.
[23] J. Yano, M. C. Noverr, P. L. Fidel, *MBio* **2017**, *8*, e00211-17.
[24] T. C. Felix, D. V. D. de Brito Röder, R. dos Santos Pedroso, *Folia Microbiol.* **2019**, *64*, 133.
[25] G. Cheng, X. Li, Z. Li, K. Zhao, G. Zhu, *J. Mol. Liq.* **2023**, *375*, 121343.
[26] A. Sugiarto, C. Kapuangan, A. R. Tantri, V. Chrisnata, *BMC Anesthesiol.* **2020**, *20*, 123.
[27] A. F. D. Di Stefano, M. M. Radicioni, A. Vaccani, G. Caccia, F. Focanti, E. Salvatori, F. Pelacchi, R. Picollo, M. T. Rosignoli, S. Olivieri, G. Bovi, A. Comandini, *Infect. Dis. Obstet. Gynecol.* **2020**, *2020*, 7201840.
[28] F. Boselli, E. Petrella, A. Campedelli, M. Muzi, V. Rullo, L. Ascione, R. Papa, G. Saponati, *ISRN Obstet. Gynecol.* **2012**, *2012*, 183403.
[29] Y. Wu, Y. Li, Y. Zou, W. Rao, Y. Gai, J. Xue, L. Wu, X. Qu, Y. Liu, G. Xu, L. Xu, Z. Liu, Z. Li, *Nano Energy* **2022**, *92*, 106715.
[30] V.-A. Duong, T.-T.-L. Nguyen, H.-J. Maeng, *Pharmaceutics* **2023**, *15*, 207.
[31] Y. Zhang, L. Huang, in *Nanoparticles Biomed. Appl*, **2020**, Elsevier, Amsterdam pp. 145.
[32] M. J. Mitchell, M. M. Billingsley, R. M. Haley, M. E. Wechsler, N. A. Peppas, R. Langer, *Nat. Rev. Drug Discovery* **2021**, *20*, 101.
[33] G. C. Carvalho, R. M. Sábio, T. de Cássia Ribeiro, A. S. Monteiro, D. V. Pereira, S. J. L. Ribeiro, M. Chorilli, *Pharm. Res.* **2020**, *37*, 191.
[34] R. Miguel Sábio, G. Corrêa Carvalho, J. Li, M. Chorilli, H. A. Santos, *Nano Sel* **2023**.
[35] A. Lérida-Viso, A. Estepa-Fernández, A. García-Fernández, V. Martí-Centelles, R. Martínez-Máñez, *Adv. Drug Delivery Rev.* **2023**, *201*, 115049.
[36] A. Noureddine, A. Maestas-Olguin, L. Tang, J. I. Corman-Hijar, M. Olewine, J. A. Krawchuck, J. Tsala Ebode, C. Edeh, C. Dang, O. A. Negrete, J. Watt, T. Howard, E. N. Coker, J. Guo, C. J. Brinker, *ACS Nano* **2023**, *17*, 16308.
[37] B. Dumontel, V. Conejo-Rodríguez, M. Vallet-Regí, M. Manzano, *Pharmaceutics* **2023**, *15*, 447.
[38] Q. Zhang, X. Chen, H. Shi, G. Dong, M. Zhou, T. Wang, H. Xin, *Colloids Surf., B* **2017**, *160*, 527.
[39] N. Han, Q. Zhao, L. Wan, Y. Wang, Y. Gao, P. Wang, Z. Wang, J. Zhang, T. Jiang, S. Wang, *ACS Appl. Mater. Interfaces* **2015**, *7*, 3342.
[40] J. Y. Choi, T. Ramasamy, S. Y. Kim, J. Kim, S. K. Ku, Y. S. Youn, J.-R. Kim, J.-H. Jeong, H.-G. Choi, C. S. Yong, J. O. Kim, *Acta Biomater.* **2016**, *39*, 94.
[41] S. J. Shepherd, D. Issadore, M. J. Mitchell, *Biomaterials* **2021**, *274*, 120826.
[42] S. Siavashy, M. Soltani, M. Ahmadi, B. Landi, H. Mehmanparast, F. Ghorbani-Bidkorbeh, *Adv. Mater. Technol.* **2022**, *7*, 2101615.

[43] M. Ahmadi, S. Siavashy, S. M. Ayyoubzadeh, R. Kecili, F. Ghorbani-Bidkorbeh, *Iran. J. Pharm. Res. IJPR* **2021**, *20*, 229.
[44] R. M. Sábio, A. B. Meneguin, A. Martins dos Santos, A. S. Monteiro, M. Chorilli, *Microporous Mesoporous Mater.* **2021**, *312*, 110774.
[45] A. Dedeloudi, A. Siamidi, P. Pavlou, M. Vlachou, *Materials* **2022**, *15*, 327.
[46] G. C. Carvalho, V. H. S. Araujo, B. Fonseca-Santos, J. T. C. de Araújo, M. P. C. de Souza, J. L. Duarte, M. Chorilli, *Int. J. Pharm.* **2021**, *602*, 120635.
[47] B. Khan, A. Arbab, S. Khan, H. Fatima, I. Bibi, N. P. Chowdhry, A. Q. Ansari, A. A. Ursani, S. Kumar, J. Hussain, S. Abdullah, *MedComm – Biomater. Appl.* **2023**, *2*, e55.
[48] M. D. Arpa, E. E. Kesmen, S. N. Biltekin, *AAPS Pharm. Sci. Tech.* **2023**, *24*, 214.
[49] A. M. dos Santos, S. G. Carvalho, V. H. S. Araujo, G. C. Carvalho, M. P. D. Gremião, M. Chorilli, *Int. J. Pharm.* **2020**, *590*, 119867.
[50] N. Prabhakar, T. Näreoja, E. von Haartman, D. Ş. Karaman, H. Jiang, S. Koho, T. A. Dolenko, P. E. Hänninen, D. I. Vlasov, V. G. Ralchenko, S. Hosomi, I. I. Vlasov, C. Sahlgren, J. M. Rosenholm, *Nanoscale* **2013**, *5*, 3713.
[51] D. Şen Karaman, G. Patrignani, E. Rosqvist, J.-H. Smått, A. Orłowska, R. Mustafa, M. Preis, J. M. Rosenholm, *Eur. J. Pharm. Sci.* **2018**, *122*, 152.
[52] D. Patra, D. Şen Karaman, D. Desai, E. El Khoury, J. M. Rosenholm, *Mater. Res. Bull.* **2016**, *84*, 267.
[53] H. Baghirov, D. Karaman, T. Viitala, A. Duchanoy, Y. R. Lou, V. Mamaeva, E. Pryazhnikov, L. Khiroug, C. De Lange Davies, C. Sahlgren, J. M. Rosenholm, *PLoS One* **2016**, *11*, e0160705.
[54] G. C. Carvalho, G. D. Marena, G. R. Leonardi, R. M. Sábio, I. Corrêa, M. Chorilli, T. M. Bauab, *Molecules* **2022**, *27*, 8558.
[55] K. Sun, T. Ding, Y. Xing, D. Mo, J. Zhang, J. M. Rosenholm, *Biomater. Sci.* **2019**, *7*, 5301.
[56] L. Ruan, W. Chen, R. Wang, J. Lu, J. I. Zink, *ACS Appl. Mater. Interfaces* **2019**, *11*, 43835.
[57] F. E. Maturi, R. M. Sábio, R. R. Silva, M. G. Lahoud, A. B. Meneguin, G. T. Valente, R. A. Caface, I. S. Leite, N. M. Inada, S. J. L. Ribeiro, *Materials* **2019**, *12*, 933.
[58] T.-H. Liou, *Carbon NY* **2004**, *42*, 785.
[59] M. Thommes, K. Kaneko, A. V. Neimark, J. P. Olivier, F. Rodriguez-Reinoso, J. Rouquerol, K. S. W. Sing, *Pure Appl. Chem.* **2015**, *87*, 1051.
[60] S. G. Ingebrigtsen, A. Didriksen, M. Johannessen, N. Škalko-Basnet, A. M. Holsæter, *Int. J. Pharm.* **2017**, *526*, 538.
[61] A. Trapani, S. Di Gioia, N. Ditaranto, N. Cioffi, F. M. Goycoolea, A. Carbone, M. Garcia-Fuentes, M. Conese, M. J. Alonso, *Int. J. Pharm.* **2013**, *447*, 115.
[62] S. Siavashy, M. Soltani, F. Ghorbani-Bidkorbeh, N. Fallah, G. Farnam, S. A. Mortazavi, F. H. Shirazi, M. H. H. Tehrani, M. H. Hamedi, *Carbohydr. Polym.* **2021**, *265*, 118027.
[63] T. M. Squires, S. R. Quake, *Rev. Mod. Phys.* **2005**, *77*, 977.
[64] D. Liu, H. Zhang, F. Fontana, J. T. Hirvonen, H. A. Santos, *Lab Chip* **2017**, *17*, 1856.
[65] D. Liu, S. Cito, Y. Zhang, C. Wang, T. M. Sikanen, H. A. Santos, *Adv. Mater.* **2015**, *27*, 2298.
[66] Y. Kim, B. L. Chung, M. Ma, W. J. M. Mulder, Z. A. Fayad, O. C. Farokhzad, R. Langer, *Nano Lett.* **2012**, *12*, 3587.
[67] Y. Ren, W. W.-F. Leung, *Int. J. Heat Mass Transf.* **2013**, *60*, 95.
[68] A. Ali, M. Wahlgren, L. Pedersen, J. Engblom, *J. Drug Deliv. Sci. Technol.* **2018**, *48*, 338.
[69] Ş. Çolak, *Radiat. Phys. Chem.* **2016**, *127*, 204.
[70] D. Sharma, R. Singh, R. Garg, *Int. J. Pharm. Sci. Res.* **2017**, *9*, 678.
[71] B. Pilicheva, Y. Uzunova, M. Marudova, *Polymers* **2022**, *14*, 734.
[72] D. Teoli, L. Parisi, N. Realdon, M. Guglielmi, A. Rosato, M. Morpurgo, *J. Controlled Release* **2006**, *116*, 295.
[73] M. Shahrousvand, N. G. Ebrahimi, H. Oliaie, M. Heydari, M. Mir, M. Shahrousvand, in *Model. Control Drug Deliv. Syst*, **2021**, Elsevier, Amsterdam pp. 45.
[74] X. Li, L. Zhang, X. Dong, J. Liang, J. Shi, *Microporous Mesoporous Mater.* **2007**, *102*, 151.
[75] S. B. Hartono, L. Hadisoewignyo, Y. Yang, A. K. Meka, Antaresti, C. Y.u, *Nanotechnology* **2016**, *27*, 505605.
[76] C. Liu, F. Jiang, Z. Xing, L. Fan, Y. Li, S. Wang, J. Ling, X.-K. Ouyang, *Pharmaceutics* **2022**, *14*, 1166.
[77] M. P. Daryasari, M. R. Akhgar, F. Mamashli, B. Bigdeli, M. Khoobi, *RSC Adv.* **2016**, *6*, 105578.
[78] P. del Pino, B. Pelaz, Q. Zhang, P. Maffre, G. U. Nienhaus, W. J. Parak, *Mater. Horiz.* **2014**, *1*, 301.
[79] V. Pareek, A. Bhargava, V. Bhanot, R. Gupta, N. Jain, J. Panwar, *J. Nanosci. Nanotechnol.* **2018**, *18*, 6653.
[80] K. Möller, T. Bein, *Chem. Mater.* **2019**, *31*, 4364.
[81] M. Wei, X. Shen, X. Fan, J. Li, J. Bai, *Front. Bioeng. Biotechnol.* **2023**, *11*, 1224339.
[82] J. P. Martins, P. Figueiredo, S. Wang, E. Espo, E. Celi, B. Martins, M. Kemell, K. Moslova, E. Mäkilä, J. Salonen, M. A. Kostiainen, C. Celia, V. Cerullo, T. Viitala, B. Sarmento, J. Hirvonen, H. A. Santos, *Bioact. Mater.* **2022**, *9*, 299.
[83] R. Cheng, L. Jiang, H. Gao, Z. Liu, E. Mäkilä, S. Wang, Q. Saiding, L. Xiang, X. Tang, M. Shi, J. Liu, L. Pang, J. Salonen, J. Hirvonen, H. Zhang, W. Cui, B. Shen, H. A. Santos, *Adv. Mater.* **2022**, *34*, 2203915.
[84] E. Ortiz-Islas, A. Sosa-Arróniz, M. E. Manríquez-Ramírez, C. E. Rodríguez-Pérez, F. Tzompantzi, J. M. Padilla, *Rev. Adv. Mater. Sci.* **2021**, *60*, 25.
[85] F. Shafiei, M. Ghavami-Lahiji, T. J. Kashi, F. Najafi, *Dent. Res. J.* **2021**, *18*, 94.
[86] N. S. Heredia, K. Vizuete, M. Flores-Calero, K. Pazmiño, V. F. Pilaquinga, B. Kumar, A. Debut, *PLoS One* **2022**, *17*, e0264825.
[87] M. Askarizadeh, N. Esfandiari, B. Honarvar, S. A. Sajadian, A. Azdarpour, *ChemBioEng Rev.* **2023**, *10*, 1006.
[88] S. Mehraji, M. Saadatmand, M. Eskandari, *Int. J. Biol. Macromol.* **2024**, *263*, 129685.
[89] S. Wang, *Microporous Mesoporous Mater.* **2009**, *117*, 1.
[90] *CLSI, M27: Reference Method for Broth Dilution Antifungal Susceptibility Testing of Yeasts; Approved Standard—4th Ed*, Clinical And Laboratory Standards Institute Wayne, PA, **2017**.
[91] G. D. Marena, G. C. Carvalho, M. A. dos Santos Ramos, M. Chorilli, T. M. Bauab, *Med. Mycol.* **2023**, *61*, myac090.
[92] S. Jebril, R. Khanfir Ben Jenana, C. Dridi, *Mater. Chem. Phys.* **2020**, *248*, 122898.
[93] O. M. Kolawole, M. T. Cook, *Eur. J. Pharm. Biopharm.* **2023**, *184*, 36.
[94] H. Bothner, O. Wik, *Acta Otolaryngol.* **1987**, *104*, 25.
[95] D. A. Adejokun, K. Dodou, *Cosmetics* **2019**, *7*, 2.
[96] C. Block, N. Watzeels, H. Rahier, B. Van Mele, G. Van Assche, *J. Therm. Anal. Calorim.* **2011**, *105*, 731.
[97] I. Rosalina, M. Bhattacharya, *Carbohydr. Polym.* **2002**, *48*, 191.
[98] F. Tuğcu-Demiröz, *Marmara Pharm. J.* **2017**, *21*, 762.
[99] S. K. Y. yaprak, S. Y. H. Karavana, P. Güneri, G. Ertan, *Pharm. Dev. Technol.* **2009**, *14*, 623.
[100] M. Mehravaran, A. Haeri, S. Rabbani, S. A. Mortazavi, M. Torshabi, *J. Drug Deliv. Sci. Technol.* **2022**, *78*, 103944.
[101] S. Dash, P. N. Murthy, L. Nath, P. Chowdhury, *Acta Polym. Pharm.* **2010**, *67*, 217.
[102] P. Trucillo, *Processes* **2022**, *10*, 1094.
[103] P. Czechowicz, J. Nowicka, G. Gościniak, *Int. J. Mol. Sci.* **2022**, *23*, 5895.
[104] F. Tacchini-Cottier, C. Zweifel, Y. Belkaid, C. Mukankundiye, M. Vasei, P. Launois, G. Milon, J. A. Louis, *J. Immunol.* **2000**, *165*, 2628.

[105] N. Nippe, G. Varga, D. Holzinger, B. Löffler, E. Medina, K. Becker, J. Roth, J. M. Ehrchen, C. Sunderkötter, *J. Invest. Dermatol.* **2011**, *131*, 125.
[106] R. Tanei, Y. Hasegawa, *Int. J. Mol. Sci.* **2022**, *23*, 6682.
[107] A. N. R, N. B. Rafiq, *Candidiasis* **2023**.
[108] M. G. de Freitas Araújo, M. Pacífico, W. Vilegas, L. C. Dos Santos, P. A. Icely, M. S. Miró, M. V. C. Scarpa, T. M. Bauab, C. E. Sotomayor, *Med. Mycol.* **2013**, *51*, 673.
[109] S. E. Navas-Alfaro, E. C. da Fonseca, M. A. Guzmán-Silva, M. C. Rochael, *J. Bras. Patol. e Med. Lab.* **2003**, *39*, 351.
[110] H. Pathave, V. Nikam, A. Dongre, U. Khopkar, *Turkish J. Dermatol.* **2022**, *16*, 38.
[111] C. Gaudiano, M. Tadolini, F. Busato, E. Vanino, S. Pucci, B. Corcioni, R. Golfieri, *Abdom. Radiol.* **2017**, *42*, 2314.
[112] P. Nyirjesy, *Curr. Infect. Dis. Rep.* **2002**, *4*, 520.
[113] L. J. Burrows, H. A. Shaw, A. T. Goldstein, *J. Sex. Med.* **2008**, *5*, 276.
[114] C. Tuoni, C. Mazzatenta, L. Filippi, *J. Pediatr.* **2023**, *260*, 113470.
[115] F. De Bernardis, M. Boccanera, R. Calderone, R. Chilar, *Mycol. Ser.* **2002**, *14*, 461.
[116] R. Pichardo-Geisinger, *Obstet. Gynecol. Clin. North Am.* **2017**, *44*, 371.
[117] A. F. Nascimento, S. R. Granter, A. Cviko, L. Yuan, J. L. Hecht, C. P. Crum, *Am. J. Surg. Pathol.* **2004**, *28*, 638.
[118] S. S. Mahalingam, S. Jayaraman, P. Pandiyan, *Pathogens* **2022**, *11*, 212.
[119] K. M. Ruaa, H. A. ALsailawi, M. M. Abdulrasool, M. Mudhafar, A. D. Mays, A. M. Bashi, *J. Life Sci.* **2021**, *15*, 10.
[120] M. A. Carrara, L. Donatti, E. Damke, T. I. E. Svidizinski, M. E. L. Consolaro, M. R. Batista, *Mycopathologia* **2010**, *170*, 331.
[121] A. Kalo-Klein, S. S. Witkin, *Am. J. Obstet. Gynecol.* **1989**, *161*, 1132.
[122] V. Känkänen, M. Fernandes, Z. Liu, J. Seitsonen, S.-P. Hirvonen, J. Ruokolainen, J. F. Pinto, J. Hirvonen, V. Balasubramanian, H. A. Santos, *J. Colloid Interface Sci.* **2023**, *633*, 383.
[123] S. L. Cerdá, F. Fontana, S. Wang, A. Correia, G. Molinaro, R. P. Tello, J. Hirvonen, C. Celia, G. Barreto, H. A. Santos, *Adv. Ther.* **2023**, *6*, 2300048.
[124] J. P. Martins, D. Liu, F. Fontana, M. P. A. Ferreira, A. Correia, S. Valentino, M. Kemell, K. Moslova, E. Mäkilä, J. Salonen, J. Hirvonen, B. Sarmento, H. A. Santos, *ACS Appl. Mater. Interfaces* **2018**, *10*, 44354.
[125] I. Arduino, Z. Liu, A. Rahikkala, P. Figueiredo, A. Correia, A. Cutrignelli, N. Denora, H. A. Santos, *Acta Biomater.* **2021**, *121*, 566.
[126] Z. Liu, W. Lian, Q. Long, R. Cheng, G. Torrieri, B. Zhang, A. Koivuniemi, M. Mahmoudzadeh, A. Bunker, H. Gao, H. He, Y. Chen, J. Hirvonen, R. Zhou, Q. Zhao, X. Ye, X. Deng, H. A. Santos, *Adv. Funct. Mater.* **2022**, *32*, 2204666.
[127] C. Tramontano, J. P. Martins, L. De Stefano, M. Kemell, A. Correia, M. Terracciano, N. Borbone, I. Rea, H. A. Santos, *Adv. Healthcare Mater.* **2023**, *12*, 2202672.
[128] P. Zhang, Y. Liu, G. Feng, C. Li, J. Zhou, C. Du, Y. Bai, S. Hu, T. Huang, G. Wang, P. Quan, J. Hirvonen, J. Fan, H. A. Santos, D. Liu, *Adv. Mater.* **2023**, *1*, 2211254.
[129] S. L. LaFayette, C. Collins, A. K. Zaas, W. A. Schell, M. Betancourt-Quiroz, A. A. L. Gunatilaka, J. R. Perfect, L. E. Cowen, *PLoS Pathog.* **2010**, *6*, e1001069.
[130] S. Kundu, U. Nithiyanantham, *RSC Adv.* **2013**, *3*, 25278.
[131] United States Pharmacopeia, <1092> The Dissolution Procedure: Development and Validation. 43–NF 38. ⟨1092⟩ The dissolution procedure: development and validation, United States Pharmacopeial Convention, United State, **2020**, 1.
[132] M. R. C. Marques, R. Loebenberg, M. Almukainzi, *Dissolution Technol.* **2011**, *18*, 15.
[133] T. Liu, X. Gong, Y. Cai, H.-Y. Li, B. Forbes, *Pharmaceutics* **2024**, *16*, 460.
[134] A. C. Apolinário, G. C. Salata, M. M. de Souza, M. Chorilli, L. B. Lopes, *AAPS PharmSciTech* **2022**, *23*, 104.
[135] P. Perlíková, A. Krajczyk, E. Doleželová, M. Slapničková, N. Milisavljevic, L. P. Slavětínská, E. Tloušťová, S. Gurská, P. Džubák, M. Hajdúch, A. Zíková, M. Hocek, *ACS Infect. Dis.* **2021**, *7*, 917.
[136] D. Duraccio, V. Strongone, G. Malucelli, F. Auriemma, C. De Rosa, F. D. Mussano, T. Genova, M. G. Faga, *Compos. Part B Eng.* **2019**, *164*, 800.
[137] T. Heikkilä, H. A. Santos, N. Kumar, D. Y. Murzin, J. Salonen, T. Laaksonen, L. Peltonen, J. Hirvonen, V.-P. Lehto, *Eur. J. Pharm. Biopharm.* **2010**, *74*, 483.
[138] S. Imlimthan, A. Correia, P. Figueiredo, K. Lintinen, V. Balasubramanian, A. J. Airaksinen, M. A. Kostiainen, H. A. Santos, M. Sarparanta, *J. Biomed. Mater. Res. Part A* **2020**, *108*, 770.
[139] N. Tahir, A. Madni, A. Correia, M. Rehman, V. Balasubramanian, M. M. Khan, H. A. Santos, *Int. J. Nanomed.* **2019**, *14*, 4961.
[140] V. H. S. Araujo, M. P. C. de Souza, G. C. Carvalho, J. L. Duarte, M. Chorilli, *Carbohydr. Polym.* **2021**, *261*, 117919.
[141] T. de C. Ribeiro, R. M. Sábio, M. T. Luiz, L. C. de Souza, B. Fonseca-Santos, L. C. Cides da Silva, M. C. de A. Fantini, C. da S. Planeta, M. Chorilli, *Pharmaceutics* **2022**, *14*, 1976.
[142] T. Carvalho, R. Bártolo, S. N. Pedro, B. F. A. Valente, R. J. B. Pinto, C. Vilela, M.-A. Shahbazi, H. A. Santos, C. S. R. Freire, *ACS Appl. Mater. Interfaces* **2023**, *15*, 25860.
[143] Z. Ahmadian, A. Correia, M. Hasany, P. Figueiredo, F. Dobakhti, M. R. Eskandari, S. H. Hosseini, R. Abiri, S. Khorshid, J. Hirvonen, H. A. Santos, M. Shahbazi, *Adv. Healthcare Mater.* **2021**, *10*, 2001122.
[144] S. Abbaszadeh, M. R. Eskandari, V. Nosrati-Siahmazgi, K. Musaie, S. Mehrabi, R. Tang, M. R. Jafari, B. Xiao, V. Hosseinpour Sarmadi, F. Haghi, B. Z. Chen, X. D. Guo, H. A. Santos, M.-A. Shahbazi, *Mater. Today Bio.* **2023**, *19*, 100609.
[145] L. Gaspar de Toledo, M. A. dos Santos Ramos, P. Bento da Silva, C. F. Rodero, V. de Sá Gomes, A. Noronha da Silva, F. R. Pavan, I. C. da Silva, F. Bombarda Oda, D. L. Flumignan, A. Gonzaga dos Santos, M. Chorilli, M. T. Gottardo de Almeida, T. M. Bauab, *Int. J. Nanomed.* **2020**, *15*, 10481.
[146] K. A. Workowski, L. H. Bachmann, P. A. Chan, C. M. Johnston, C. A. Muzny, I. Park, H. Reno, J. M. Zenilman, G. A. Bolan, *MMWR. Recomm. Rep. Morb. Mortal. Wkly. Rep. Recomm. Rep.* **2021**, *70*, 1.
[147] L. P. Quintella, S. R. Lambert Passos, A. C. Francesconi do Vale, M. C. Gutierrez Galhardo, M. B. De Lima Barros, T. Cuzzi, R. Dos Santos Reis, M. H. G. Figueiredo de Carvalho, M. B. Zappa, A. De Oliveira Schubach, *J. Cutan. Pathol.* **2011**, *38*, 25.